Generalization of the phase-screen approximation for the scattering of acoustic waves

MAARTEN V. DE HOOP , JÉRÔME H. LE ROUSSEAU
Center for Wave Phenomena,
Colorado School of Mines,
Golden CO 80401-1887, USA
AND
RU-SHAN WU
Institute of Tectonics,
University of California,
Santa Cruz CA 95064, USA

June 30, 1999

Abstract

With the use of Fourier analysis, we describe the propagation and scattering of acoustics waves in smoothly varying, heterogeneous, media. The starting point is the generalized Bremmer coupling series solution – distinguishing multiple up/down scattered constituents – to the wave equation, which requires the introduction of pseudo-differential operators. Then, we introduce a class of approximations to these pseudo-differential operators with the structure of the classical phase-screen method for one-way wave propagation. These approximations induce a fast, iterated, marching algorithm for the evaluation of the Bremmer series. The algorithm consists of multiplications by multiple 'screen' functions in the lateral space domain and generalized 'phase shifts' in the lateral wavenumber domain; the shuttling between the two domains is accomplished by the fast Fourier transform. Our scheme extends the use of the classical phase-screen method in the following ways: we consider larger medium variations; we enhance the accuracy for wider scattering angles; we introduce (de)composition operators to incorporate any desired source- or receiver-type with the appropriate radiation characteristics; we include the backscattered field with the aid of the generalized Bremmer coupling series.

1 Introduction

Directional wavefield decomposition is a tool for analyzing and computing the propagation of waves in configurations with a certain directionality, such as waveguiding structures. The method consists of three main steps: (i) *decomposing* the field into two constituents, *propagating* upward or downward along a preferred direction, (ii) computing the interaction (*coupling*) of the counterpropagating constituents and (iii) *recomposing* the constituents into observables at the positions of interest. (The preferred direction is 'vertical' whereas the directions orthogonal to the preferred direction are referred to as the 'lateral' directions.) The method allows one to 'trace' wave constituents in a given medium, and thus distinguish constituents that have been scattered along the up/down direction a different number of times. It allows the separation of head waves from body waves also. The (generalized) Bremmer series superimposes all the constituents ('multiples') to recover the full, original wavefield (De Hoop [1]).

In the framework of remote sensing and inverse scattering, tracing waves helps in the interpretation and separation of constituents prior to the inversion of the observed wavefield (De Hoop [2]). Directional decomposition maps the 'two-way' wavefield into constituents that satisfy a coupled system of 'one-way' wave equations. In large-scale configurations in which the coupling is weak, wavefield computations can be restricted to a single one-way constituent. In the fields of ocean acoustics (Tappert [3], Collins [4]), seismics (Claerbout [5]), and integrated optics (Hadley [6]), this observation has been exploited extensively; for a more complete list of references in this matter, we refer the reader to Van Stralen *et al.* [7]. However, to arrive at 'fast' one-way algorithms in the mentioned applications, various approximations to the decomposition underly their designs.

If the medium of the configuration were laterally homogeneous, the directional decomposition becomes an algebraic operation in the lateral Fourier or wavenumber domain (see, e.g., Kennett [8]). In such a medium, the phase-shift method (Gazdag [9]) is amongst the fastest (and accurate) one-way algorithms. In this method, in the lateral wavenumber domain, the phase shift is simply proportional to the vertical wavenumber; the vertical and lateral wavenumbers are connected through an algebraic dispersion relation. As soon as the medium becomes laterally heterogenous, it still advantageous to carry out the analysis in the lateral wavenumber domain, but without leaving the lateral space domain – an observation well established in the field of micro-local analysis (see, e.g., Treves [10]) and applied by Fishman and McCoy [11]. The lateral space-wavenumber domain constitutes the (lateral) phase space. Through the Fourier transforms, the space and wavenumber domains are 'dual' to one another. In the directional (de)composition – and in the downward and upward propagation, and in the reflection and

transmission due to variations in medium properties in the preferred direction – we now encounter pseudo-differential operators the symbols of which are defined on phase space, and lead to a calculus that generalizes the algebraic manipulations in the case of a laterally homogeneous medium (De Hoop [1] and Section 2). Unfortunately, numerical evaluation and application of pseudo-differential operators arising from the wave scattering problem are, in general, involved. Hence, approximations to their symbols are sought for to improve computational efficiency. The phase-screen method (Stoffa *et al.* [12] and Wu and Huang [13]) provides one such approximation and leads to an algorithm with computational complexity comparable to the one of the phase-shift method in laterally homogeneous media. A competing approximation is the rational one, analyzed in detail by De Hoop and De Hoop [14] and Van Stralen *et al.* [7].

The reason why the phase-screen approximation leads to an efficient algorithm is, that its associated symbols reveal a separation of phase-space coordinates. We will use this observation as the starting point for developing a general class of approximations: the *generalized screen* approximations. It comprises *enforcing* in the symbols of the pseudo-differential operators that generate the generalized Bremmer series, a *separation* of phase-space coordinates. The one-way algorithm, inside the Bremmer series, yields an approximate realization of the phase-space path-integral representation for one-way propagation (Fishman and McCoy [15], De Hoop [1]); the Hamiltonian of this path integral is the vertical wave slowness (vertical wavenumber divided by frequency) symbol subjected to the separation of phase-space coordinates (Section 3). Now, the vertical wave slowness and the lateral wave slownesses are connected through a symbol composition equation. The path integral extends the phase-shift operation to laterally heterogeneous media; its generalized screen realization is founded upon a continuous shuttling between the lateral space and lateral wavenumber domains using the fast Fourier transform (Section 5).

Subjecting the symbols, in particular the vertical wave slowness symbol, to the separation of phase-space coordinates, induces an 'adjustment' of wave theory and deformations of the wavefront shapes. The accuracy of the generalized screen approximations is most accessible in phase space by analyzing the (approximate) vertical wave slowness symbols as functions of the lateral wave slownesses (lateral wavenumbers) pointwise in lateral space. In the high-frequency approximation, i.e. up to principal symbols, these functions generate the slowness surface, the polar reciprocal of which creates the Huygens wavefront (Section 5). In Section 6 we discuss the generalized screen representations of (de)composition; in Section 7 we introduce the generalized screen representations of reflection and transmission. The marching algorithm associated with the generalized Bremmer series and leading to the wavefield solution

is summarized in Section 4; in this algorithm, the thin-slab propagator of Section 5, the reflection and transmission operators of Section 7, and the (de)composition operators of Section 6 are to be substituted.

A framework of marching algorithms and path integrals for wave propagation has been established by McCoy and Frazer [16]. The method of phase screens has been widely used for one-way wave propagation in *smoothly* varying, heterogeneous media. In particular, the method has been applied to light transmission through the atmosphere (Ratcliffe [17], Mercier [18], and Martin and Flatté [19]), propagation of light in optical fibers (Feit and Fleck [20]), propagation of radio signals through the ionosphere (Buckley [21], Bramley [22], Knepp [23]), propagation of acoustic waves in the ocean (Flatté [24], Thomson and Chapman [25]), and propagation of seismic waves in the earth (Stoffa *et al.* [12]). More recently, the screen method has been introduced for elastic waves (Fisk and McCartor [26], Fisk *et al.* [27], and Wu [28]). The phase-screen approach has also been applied in media that are not smoothly varying at all: Berry [29] analyzed the intensity fluctuations of an incident plane wave scattered in a *fractal* medium.

Classically, the phase-screen method was designed for multiple downward scattering of waves, the downward direction being the preferred direction of propagation. Thus it included phenomena like focussing and defocussing i.e. 'multipathing' of the characteristic set. The applicability of the phase-screen method generally requires that the screen interval satisfies the following criteria: small medium variations (weak scattering), laterally smooth medium variations (narrow angle scattering), and even smoother variations in the preferred direction (negligible backscattering). In this paper, we access the accuracy of the screen method, and generalize it to larger-contrast (larger range of medium variations within a screen interval), wider-angle, and back scattering. The higher the order of the generalized screen approximation, the more parameters occur that shape the wavefront. The order controls the accuracy.

Given the order of the generalized screen approximation, its accuracy can still be enhanced by replacing the (fast) lateral Fourier transform by a *windowed* lateral Fourier transform, the windows following an imprint of the major lateral changes in medium properties (Section 5). One may wonder whether the underlying windowed, lateral Fourier basis could be even further improved upon. De Hoop and Gautesen [30] have accomplished such an improvement, incorporating all one-way wave phenemona, at the cost of computational efficiency.

2 Directional wavefield decomposition

For the details on the derivation of the Bremmer coupling series solution of the acoustic wave equation, we refer the reader to De Hoop [1]. Here, we restrict ourselves to a summary of the method. Our configuration is three-dimensional.

Let p = acoustic pressure [Pa], v_r = particle velocity [m/s], ρ = volume density of mass [kg/m^3], κ = compressibility [Pa^{-1}], q = volume source density of injection rate [s^{-1}], and f_k = volume source density of force [N/m^3]. We assume that the coefficients κ and ρ are smooth, and constant outside a compact domain. This provision enables us to formulate the acoustic wave propagation, when necessary, as a scattering problem in a homogeneous embedding. The smoothness entails that the singularities of the wavefield (in particular the ones in the neighborhood of the wave arrival) arise from the ones in the signatures of the source distributions. The formation of caustics, associated with scattering in the lateral directions ('multipathing'), is captured in the approximation procedure developed in this paper.

We carry out our analysis in the time-Laplace domain. To show the notation, we give the expression for the acoustic pressure,

$$\hat{p}(x_m, s) = \int_{t=0}^{\infty} \exp(-st) p(x_m, t)\, \mathrm{d}t \ . \tag{2.1}$$

Under this transformation, assuming zero initial conditions, we have $\partial_t \to s$. In the Laplace domain, the acoustic wavefield satisfies the system of first-order equations

$$\partial_k \hat{p} + s\rho\, \hat{v}_k = \hat{f}_k \ , \tag{2.2}$$

$$s\kappa\, \hat{p} + \partial_r \hat{v}_r = \hat{q} \ . \tag{2.3}$$

The evolution of the wavefield in the direction of preference can now be expressed in terms of the changes of the wavefield in the direction transverse to it. The direction of preference is taken along the x_3-axis (or 'vertical' axis) and the remaining ('lateral' or 'horizontal') coordinates are denoted by x_μ, $\mu = 1, 2$.

Since we allow the medium to vary with all coordinates and hence also with coordinate in the preferred direction, we are forced to carry out the wavefield decomposition from the system of first-order equations rather than the second-order scalar 'Helmholtz' equation.

The reduced system of equations

The decomposition procedure requires a separate handling of the horizontal components of the particle velocity. From Eqs.(2.2) and (2.3) we obtain

$$\hat{v}_\mu = -\rho^{-1}s^{-1}(\partial_\mu \hat{p} - \hat{f}_\mu) \ , \tag{2.4}$$

leaving, upon substitution, the matrix differential equation

$$(\partial_3 \delta_{I,J} + s\hat{A}_{I,J})\hat{F}_J = \hat{N}_I \ , \quad \hat{A}_{I,J} = \hat{A}_{I,J}(x_\mu, D_\nu; x_3) \ , \quad D_\nu \equiv -\frac{1}{s}\partial_\nu \ , \tag{2.5}$$

in which $\delta_{I,J}$ is the Kronecker delta, and the elements of the acoustic field matrix are given by

$$\hat{F}_1 = \hat{p} \ , \quad \hat{F}_2 = \hat{v}_3 \ , \tag{2.6}$$

the elements of the acoustic system's operator matrix by

$$\hat{A}_{1,1} = \hat{A}_{2,2} = 0 \ , \tag{2.7}$$

$$\hat{A}_{1,2} = \rho \ , \tag{2.8}$$

$$\hat{A}_{2,1} = -D_\nu(\rho^{-1}D_\nu \,) + \kappa \ , \tag{2.9}$$

and the elements of the notional source matrix by

$$\hat{N}_1 = \hat{f}_3 \ , \quad \hat{N}_2 = D_\nu(\rho^{-1}\hat{f}_\nu) + \hat{q} \ . \tag{2.10}$$

It is observed that the right-hand side of Eq.(2.4) and $\hat{A}_{I,J}$ contain the spatial derivatives D_ν with respect to the horizontal coordinates only. D_ν has the interpretation of *horizontal slowness* operator. Further, it is noted that $\hat{A}_{1,2}$ is simply a multiplicative operator.

The coupled system of one-way wave equations

To distinguish up- and downgoing constituents in the wavefield, we shall construct an appropriate linear operator $\hat{L}_{I,J}$ with

$$\hat{F}_I = \hat{L}_{I,J}\hat{W}_J \ , \tag{2.11}$$

that, with the aid of the commutation relation $(\partial_3 \hat{L}_{I,J}) = [\partial_3, \hat{L}_{I,J}]$, transforms Eq.(2.5) into

$$\hat{L}_{I,J}\,(\partial_3 \delta_{J,M} + s\hat{\Lambda}_{J,M})\hat{W}_M = -(\partial_3 \hat{L}_{I,J})\,\hat{W}_J + \hat{N}_I \ , \tag{2.12}$$

as to make $\hat{\Lambda}_{J,M}$, satisfying

$$\hat{A}_{I,J}\hat{L}_{J,M} = \hat{L}_{I,J}\hat{\Lambda}_{J,M} \ , \tag{2.13}$$

a diagonal matrix of operators. We denote $\hat{L}_{I,J}$ as the composition operator and $\hat{W}_M$ as the wave matrix. The matrix expression in parentheses on the left-hand side of Eq.(2.12) is diagonal and its diagonal entries are the two so-called *one-way* wave operators. The first term on the right-hand side of Eq.(2.12) is representative for the scattering due to variations of the medium properties in the vertical direction. The scattering due to variations of the medium properties in the horizontal directions is contained in $\hat{\Lambda}_{J,M}$ and, implicitly, in $\hat{L}_{I,J}$ also.

To investigate whether solutions of Eq.(2.13) exist, we introduce the column matrix operators $\hat{L}_I^{(\pm)}$ according to

$$\hat{L}_I^{(+)} = \hat{L}_{I,1} \ , \quad \hat{L}_I^{(-)} = \hat{L}_{I,2} \ . \tag{2.14}$$

Upon writing the diagonal entries of $\hat{\Lambda}_{J,M}$ as

$$\hat{\Lambda}_{1,1} = \hat{\Gamma}^{(+)} \ , \quad \hat{\Lambda}_{2,2} = \hat{\Gamma}^{(-)} \ , \tag{2.15}$$

Eq.(2.13) decomposes into the two systems of equations

$$\hat{A}_{I,J}\hat{L}_J^{(\pm)} = \hat{L}_I^{(\pm)}\hat{\Gamma}^{(\pm)} \ . \tag{2.16}$$

By analogy with the case where the medium is translationally invariant in the horizontal directions, we shall denote $\hat{\Gamma}^{(\pm)}$ as the *vertical slowness* operators. Notice that the operators $\hat{L}_1^{(\pm)}$ compose the acoustic pressure and that the operators $\hat{L}_2^{(\pm)}$ compose the vertical particle velocity from the elements of $\hat{W}_M$ associated with the up- and downgoing constituents.

In De Hoop [1] an Ansatz procedure has been followed to solve the generalized eigenvalue-eigenvector problem (2.16) in operator sense: choosing the *acoustic-pressure normalization* analog, we satisfy the commutation rule

$$[\hat{L}_2^{(\pm)}, \hat{A}_{2,1}\hat{A}_{1,2}] = 0 \ . \tag{2.17}$$

In this normalization, we find the vertical slowness operator or generalized eigenvalues to be

$$\hat{\Gamma}^{(+)} = -\hat{\Gamma}^{(-)} = \hat{\Gamma} = \hat{\mathrm{A}}^{1/2} \ , \quad \hat{\mathrm{A}} \equiv \hat{A}_{2,1}\hat{A}_{1,2} \ ; \quad \hat{\Gamma}^2 = \hat{\mathrm{A}} \tag{2.18}$$

is the characteristic operator equation, while the generalized eigenvectors constitute the *composition* operator

$$\hat{L} = \begin{pmatrix} \hat{A}_{1,2} & \hat{A}_{1,2} \\ \hat{\Gamma} & -\hat{\Gamma} \end{pmatrix} \ . \tag{2.19}$$

With respect to the normalization, note that we have decomposed the *pressure* (up to a multiplication by density) viz. according to $\hat{F}_1 = \hat{F}_1^+ + \hat{F}_1^-$, $\hat{F}_1^+ = \hat{A}_{1,2}\hat{W}_1$ and $\hat{F}_1^- = \hat{A}_{1,2}\hat{W}_2$.

In terms of the inverse vertical slowness operator, $\hat{\Gamma}^{-1} = \hat{\mathrm{A}}^{-1/2}$, the *decomposition* operator then follows as

$$\hat{L}^{-1} = \tfrac{1}{2}\begin{pmatrix} \hat{A}_{1,2}^{-1} & \hat{\Gamma}^{-1} \\ \hat{A}_{1,2}^{-1} & -\hat{\Gamma}^{-1} \end{pmatrix} . \tag{2.20}$$

The (de)composition operators account for the radiation patterns of the different source and receiver types.

Using the decomposition operator, Eq.(2.12) transforms into

$$(\partial_3\delta_{I,M} + s\hat{\Lambda}_{I,M})\hat{W}_M = -(\hat{L}^{-1})_{I,M}(\partial_3\hat{L}_{M,K})\hat{W}_K + (\hat{L}^{-1})_{I,M}\hat{N}_M , \tag{2.21}$$

which can be interpreted as a coupled system of one-way wave equations. The coupling between the counter-propagating components, $\hat{W}_1$ and $\hat{W}_2$, is apparent in the first source-like term on the right-hand side, which can be written as

$$-\hat{L}^{-1}(\partial_3\hat{L}) = \begin{pmatrix} \hat{T} & \hat{R} \\ \hat{R} & \hat{T} \end{pmatrix} , \tag{2.22}$$

in which $\hat{T}$ and $\hat{R}$ represent the *transmission* and *reflection* operators, respectively. In the acoustic-pressure normalization analog, we find

$$-\hat{T} = \tfrac{1}{2}\hat{A}_{1,2}^{-1}(\partial_3\hat{A}_{1,2}) + \tfrac{1}{2}\hat{\Gamma}^{-1}(\partial_3\hat{\Gamma}) , \ \hat{R} = -\tfrac{1}{2}\hat{A}_{1,2}^{-1}(\partial_3\hat{A}_{1,2}) + \tfrac{1}{2}\hat{\Gamma}^{-1}(\partial_3\hat{\Gamma}) . \tag{2.23}$$

3 The one-way wave propagator

To arrive at a coupled system of integral equations that is equivalent to Eq.(2.21) and that can be solved in terms of a Neumann expansion, we have to invert the operator occurring on the left-hand side. We set $\hat{\mathrm{G}}^{(\pm)} = (\partial_3 + s\hat{\Gamma}^{(\pm)})^{-1}$. The one-sided elementary kernels $\hat{\mathcal{G}}^{(\pm)}(x_\mu, x_3; x'_\nu, x'_3)$ associated with these operators are the so-called one-way Green's functions. They satisfy the equations

$$(\partial_3 + s\hat{\Gamma}^{(\pm)})\hat{\mathcal{G}}^{(\pm)} = \delta(x_\nu - x'_\nu)\,\delta(x_3 - x'_3) , \tag{3.1}$$

together with the condition of causality enforcing that $\hat{\mathcal{G}}^{(\pm)}$ decays as $x_3 \to \pm\infty$.

Now, consider the case $\hat{\mathrm{G}} = \hat{\mathrm{G}}^{(+)}$, $\hat{\mathcal{G}} = \hat{\mathcal{G}}^{(+)}$ and $\hat{\Gamma} = \hat{\Gamma}^{(+)}$. The operator $\hat{\mathrm{G}}$ acts on a test field $\hat{u}$ as

$$(\hat{\mathrm{G}}\hat{u})(x_\mu, x_3) = \int_{\zeta\in\mathbb{R}} \int_{x'_\nu\in\mathbb{R}} \hat{\mathcal{G}}(x_\mu, x_3; x'_\nu, \zeta)\, \hat{u}(x'_\nu, \zeta)\, \mathrm{d}x'_1 \mathrm{d}x'_2\, \mathrm{d}\zeta\ . \tag{3.2}$$

Let us define the initial-value problem of determining the function $\hat{U}(x_\mu, x_3; \zeta)$ satisfying

$$(\partial_3 + s\hat{\Gamma})\, \hat{U} = 0 \text{ for } x_3 \geq \zeta,\ \ \hat{U}(x_\mu, \zeta; \zeta) = \hat{u}(x_\mu, \zeta)\ . \tag{3.3}$$

Then it is observed that

$$(\hat{\mathrm{G}}\hat{u})(x_\mu, x_3) = \int_{\zeta=-\infty}^{x_3} \hat{U}(x_\mu, x_3; \zeta)\, \mathrm{d}\zeta\ . \tag{3.4}$$

The product integral

We note that the vertical slowness operators at different levels of x_3 do not necessarily commute with one another due to the heterogeneity of the medium. Thus we arrive at a 'time'-ordered product integral representation [31] of the one-sided propagators (cf. Eq.(3.3)) associated with the one-way wave equations [1, 11, 15] where 'time' refers to the vertical coordinate x_3,

$$\hat{U}^{(\pm)}(., x_3; x'_3) = \pm H(\mp[x'_3 - x_3]) \left\{ \prod_{\zeta=x'_3}^{x_3} \exp[-s\hat{\Gamma}^{(\pm)}(., \zeta)\, \mathrm{d}\zeta] \right\} \hat{u}(., x'_3)\ , \tag{3.5}$$

where H denotes the Heaviside function. In this expression, the operator ordering is initiated by $\exp[-s\hat{\Gamma}(., x'_3)\, \mathrm{d}\zeta]$ acting on $\hat{u}(., x'_3)$ followed by applying $\exp[-s\hat{\Gamma}(., \zeta)\, \mathrm{d}\zeta]$ to the result, successively for increasing ζ.

If the medium in the interval $[x'_3, x_3]$ were weakly varying in the vertical direction, the Trotter product formula can be applied to the product integral in Eq.(3.5). This results in the Hamiltonian path integral representations [31] with measure $\mathcal{D}$ for the Green's functions,

$$\hat{\mathcal{G}}^{(\pm)}(x_\mu, x_3; x'_\nu, x'_3) = \pm H(\mp[x'_3 - x_3]) \int_P \mathcal{D}(x''_\mu, \alpha''_\nu) \tag{3.6}$$

$$\exp\left[-s \int_{\zeta=x'_3}^{x_3} \mathrm{d}\zeta \{\mathrm{i}\alpha''_\sigma(d_\zeta x''_\sigma) + \hat{\gamma}^{(\pm)}(x''_\mu, \zeta, \alpha''_\nu)\}\right] = \pm H(\mp[x'_3 - x_3])\, \hat{g}^{(\pm)}(x_\mu, x_3; x'_\nu, x'_3)\ ,$$

P being a set of paths $(x''_\mu(\zeta), \alpha''_\nu(\zeta))$ in (horizontal) phase space satisfying $x''_\mu(\zeta = x'_3) = x'_\mu\ ,\ x''_\mu(\zeta = x_3) = x_\mu$. In Eq.(3.6), $\hat{\gamma}^{(\pm)}$ is the left symbol of $\Gamma^{(\pm)}$, i.e.

$$\hat{\Gamma}^{(\pm)}(x_\mu, D_\nu; \zeta)\ \exp(-\mathrm{i}s\alpha_\sigma x_\sigma) = \hat{\gamma}^{(\pm)}(x_\mu, \zeta, \alpha_\nu) \exp(-\mathrm{i}s\alpha_\sigma x_\sigma)\ . \tag{3.7}$$

The path integral in Eq.(3.6) is to be interpreted as the lattice multi-variate integral

$$\hat{\mathcal{G}}^{(\pm)}(x_\mu,x_3;x'_\nu,x'_3)=\pm H(\mp[x'_3-x_3])\lim_{M\to\infty}\int\prod_{i=1}^{M}(s/2\pi)^2\mathrm{d}\alpha_1^{(i)}\mathrm{d}\alpha_2^{(i)}\prod_{j=1}^{M-1}\mathrm{d}x_1^{(j)}\mathrm{d}x_2^{(j)}$$

$$\exp\left[-s\sum_{k=1}^{M}\{\mathrm{i}\alpha_\sigma^{(k)}(x_\sigma^{(k)}-x_\sigma^{(k-1)})+\hat{\gamma}^{(\pm)}(x_\mu^{(k)},\zeta_k-\tfrac{1}{2}M^{-1}\Delta x_3,\alpha_\nu^{(k)})M^{-1}\Delta x_3\}\right] \tag{3.8}$$

with $x_\mu^{(0)}=x'_\mu$, $x_\mu^{(M)}=x_\mu$, and $\Delta x_3=x_3-x'_3$. All the integrations are taken over the interval $(-\infty,\infty)$, $M^{-1}\Delta x_3$ is the step size in ζ, and $(x_\mu^{(j)},\alpha_\nu^{(j)})$ are the coordinates of a path at the discrete values ζ_j of ζ as $j=1,\cdots,M$.

The thin-slab propagator

If Δx_3 is sufficiently small (thin slab), the lattice multi-variate integral reduces to ($M=1$)

$$\hat{g}^{(\pm)}(x_\mu,x_3;x'_\nu,x'_3)\simeq\int(s/2\pi)^2\mathrm{d}\alpha''_1\mathrm{d}\alpha''_2$$
$$\exp[-\mathrm{i}s\,\alpha''_\sigma(x_\sigma-x'_\sigma)]\exp[-s\,\hat{\gamma}^{(\pm)}(x_\mu,x_3-\tfrac{1}{2}\Delta x_3,\alpha''_\nu)\Delta x_3]\;. \tag{3.9}$$

Thus, thin-slab propagation is composed of a forward Fourier transform, a multiplication by a phase factor (the phase is the vertical slowness left symbol) and an inverse Fourier transform. Switching from left to right symbols[1] yields

$$\hat{g}^{(\pm)}(x_\mu,x_3;x'_\nu,x'_3)\simeq\int(s/2\pi)^2\mathrm{d}\alpha''_1\mathrm{d}\alpha''_2$$
$$\exp[-\mathrm{i}s\,\alpha''_\sigma(x_\sigma-x'_\sigma)]\exp[-s\,\hat{\gamma}^{(\pm)}(x'_\nu,x_3-\tfrac{1}{2}\Delta x_3,\alpha''_\nu)\Delta x_3]\;. \tag{3.10}$$

With the vertical slowness left symbol is associated a cokernel

$$\tilde{\gamma}(\alpha_\mu,\zeta,\alpha'_\nu)=\int_{x_\mu\in\mathbb{R}}\exp(\mathrm{i}s\alpha_\mu x_\mu)\,\hat{\gamma}(x_\mu,\zeta,\alpha'_\nu)\,\mathrm{d}x_1\mathrm{d}x_2\;. \tag{3.11}$$

Thus, in the Fourier domain, the thin slab propagator can written in the form (cf. Eq.(3.9)),

$$\tilde{g}^{(\pm)}(\alpha_\mu,x_3;\alpha''_\nu,x'_3)\simeq\int\mathrm{d}x_1\mathrm{d}x_2$$
$$\exp[\mathrm{i}s\,(\alpha_\sigma-\alpha''_\sigma)\,x_\sigma]\exp[-s\,\hat{\gamma}^{(\pm)}(x_\mu,x_3-\tfrac{1}{2}\Delta x_3,\alpha''_\nu,s)\Delta x_3]\;, \tag{3.12}$$

[1]The right or *dual* symbol $\hat{\gamma}_{\mathrm{R}}$ is related to the *left* symbol $\hat{\gamma}$ according to $\hat{\gamma}_{\mathrm{R}}(x_\mu,\zeta,\alpha_\nu)\sim\exp[\mathrm{i}\,\partial_{\alpha_\sigma}D_{x_\sigma}]\,\hat{\gamma}(x_\mu,\zeta,\alpha_\nu)$. We will omit the subscript $_{\mathrm{R}}$ whenever it is clear from the context which symbol is meant.

and may, for small Δx_3, be approximated by

$$\tilde{g}^{(\pm)}(\alpha_\mu, x_3; \alpha''_\nu, x'_3) \simeq \delta(\alpha_\mu - \alpha''_\mu) - s\,\tilde{\gamma}^{(\pm)}(\alpha_\mu - \alpha''_\mu, x_3 - \tfrac{1}{2}\Delta x_3, \alpha''_\nu, s)\Delta x_3 + \cdots \ . \quad (3.13)$$

This representation shows the interaction of Fourier constituents $\exp(-\mathrm{i}s\alpha_\sigma x_\sigma)$ explicitly.

4 The generalized Bremmer coupling series

The coupled system of integral equations

Applying the operators with kernels Eq.(3.6) to Eq.(2.21) we obtain a coupled system of integral equations (De Hoop [1]). In operator form, they are given by

$$(\delta_{I,J} - \hat{\mathrm{K}}_{I,J})\hat{W}_J = \hat{W}_I^{(0)} \ , \quad (4.1)$$

in which $\hat{W}^{(0)}$ denotes the incident field. In our configuration the domain of heterogeneity will be restricted to the slab $(0, x_3^{\mathrm{exit}}]$, and the excitation of the waves will be specified through an initial condition at the level $x_3 = 0$, viz.

$$\hat{W}_1^{(0)}(x_\mu, x_3) = \int_{x'_\nu \in \mathbb{R}} \hat{\mathcal{G}}^{(+)}(x_\mu, x_3; x'_\nu, 0)\, \hat{W}_1(x'_\nu, 0)\, \mathrm{d}x'_1\, \mathrm{d}x'_2 \ , \quad (4.2)$$

$$\hat{W}_2^{(0)}(x_\mu, x_3) = 0 \ , \quad (4.3)$$

in the range of interest, $x_3 \in [0, x_3^{\mathrm{exit}}]$; the second equation reflects the assumption that there is no excitation below the heterogeneous slab. The integral operators in Eq.(4.1) are given by

$$(\hat{\mathrm{K}}_{1,1}\hat{W}_1)(x_\mu, x_3) = \int_{\zeta=0}^{x_3} \int_{x'_\nu \in \mathbb{R}} \hat{\mathcal{G}}^{(+)}(x_\mu, x_3; x'_\nu, \zeta)(\hat{T}\hat{W}_1)(x'_\nu, \zeta)\, \mathrm{d}x'_1\, \mathrm{d}x'_2\, \mathrm{d}\zeta \ , \quad (4.4)$$

$$(\hat{\mathrm{K}}_{1,2}\hat{W}_2)(x_\mu, x_3) = \int_{\zeta=0}^{x_3} \int_{x'_\nu \in \mathbb{R}} \hat{\mathcal{G}}^{(+)}(x_\mu, x_3; x'_\nu, \zeta)(\hat{R}\hat{W}_2)(x'_\nu, \zeta)\, \mathrm{d}x'_1\, \mathrm{d}x'_2\, \mathrm{d}\zeta \ , \quad (4.5)$$

$$(\hat{\mathrm{K}}_{2,1}\hat{W}_1)(x_\mu, x_3) = \int_{\zeta=x_3}^{x_3^{\mathrm{exit}}} \int_{x'_\nu \in \mathbb{R}} \hat{\mathcal{G}}^{(-)}(x_\mu, x_3; x'_\nu, \zeta)(\hat{R}\hat{W}_1)(x'_\nu, \zeta)\, \mathrm{d}x'_1\, \mathrm{d}x'_2\, \mathrm{d}\zeta \ , \quad (4.6)$$

$$(\hat{\mathrm{K}}_{2,2}\hat{W}_2)(x_\mu, x_3) = \int_{\zeta=x_3}^{x_3^{\mathrm{exit}}} \int_{x'_\nu \in \mathbb{R}} \hat{\mathcal{G}}^{(-)}(x_\mu, x_3; x'_\nu, \zeta)(\hat{T}\hat{W}_2)(x'_\nu, \zeta)\, \mathrm{d}x'_1\, \mathrm{d}x'_2\, \mathrm{d}\zeta \ . \quad (4.7)$$

They describe the interaction between the counter-propagating constituent waves.

We can represent the action of the one-sided Green's kernels by product integrals, viz.,

$$\hat{W}_1^{(0)}(.,x_3) = \left\{ \prod_{\zeta'=0}^{x_3} \exp[-s\hat{\Gamma}^{(+)}(.,\zeta')\,\mathrm{d}\zeta'] \right\} \hat{W}_1(.,0)\ , \tag{4.8}$$

while

$$(\hat{\mathrm{K}}_{1,1}\hat{W}_1)(.,x_3) = \int_{\zeta=0}^{x_3} \left\{ \prod_{\zeta'=\zeta}^{x_3} \exp[-s\hat{\Gamma}^{(+)}(.,\zeta')\,\mathrm{d}\zeta'] \right\} (\hat{T}\hat{W}_1)(.,\zeta)\,\mathrm{d}\zeta\ , \tag{4.9}$$

and so on.

Bremmer series

If s is real and sufficiently large, the Neumann expansion can be employed to invert $(\delta_{I,J}-\hat{\mathrm{K}}_{I,J})$ in Eq.(4.1). Such a procedure leads to the Bremmer coupling series,

$$\hat{W}_I = \sum_{j=0}^{\infty} \hat{W}_I^{(j)}\ , \qquad \text{in which } \hat{W}_I^{(j)} = \hat{\mathrm{K}}_{I,J}\hat{W}_J^{(j-1)} \text{ for } j \geq 1\ , \tag{4.10}$$

can be interpreted as the j-times reflected or scattered wave. This equation indicates that the solution of Eq.(4.1) can be found with the aid of an iterative scheme. This iterative scheme and its computational aspects are discussed in detail by Van Stralen *et al.* [7, III.C]. On the basis of Lerch's theorem [32], we only need the individual terms for s on some real half line to get back to the time domain; the earlier condition 'sufficiently large' does not play any role in this respect.

An iterated marching algorithm

To arrive at a marching algorithm nested in an iterative scheme, consider the j-times reflected constituent wave. We split the interval $[0, x_3^{\mathrm{exit}}]$ into M thin slabs with thickness Δx_3. Set

$$\hat{W}_I^{(j)}(.,k\Delta x_3) = \hat{I}_{I,1}^{(j)}(.,k) + \hat{I}_{I,2}^{(j)}(.,k)\ , \tag{4.11}$$

$j = 1, 2, \cdots$ and $k = 0, 1, \cdots, M$, where (cf. Eq.(4.10))

$$\hat{I}_{I,1}^{(j)}(.,k) = (\hat{\mathrm{K}}_{I,1}\hat{W}_1^{(j-1)})(.,k\Delta x_3)\ , \tag{4.12}$$

$$\hat{I}_{I,2}^{(j)}(.,k) = (\hat{\mathrm{K}}_{I,2}\hat{W}_2^{(j-1)})(.,k\Delta x_3)\ . \tag{4.13}$$

Upon comparison with Eq.(4.9) we find that

$$\hat{I}^{(j)}_{1,1}(.,k) = \int_{\zeta=0}^{k\Delta x_3} \left\{ \prod_{\zeta'=\zeta}^{k\Delta x_3} \exp[-s\hat{\Gamma}^{(+)}(.,\zeta')\,\mathrm{d}\zeta'] \right\} \hat{X}^{(j)}_{1,1}(.,\zeta)\,\mathrm{d}\zeta \ , \tag{4.14}$$

with

$$\hat{X}^{(j)}_{1,1}(.,\zeta) = (\hat{T}\hat{W}^{(j-1)}_1)(.,\zeta) \ . \tag{4.15}$$

Similarly,

$$\hat{I}^{(j)}_{1,2}(.,k) = \int_{\zeta=0}^{k\Delta x_3} \left\{ \prod_{\zeta'=\zeta}^{k\Delta x_3} \exp[-s\hat{\Gamma}^{(+)}(.,\zeta')\,\mathrm{d}\zeta'] \right\} \hat{X}^{(j)}_{1,2}(.,\zeta)\,\mathrm{d}\zeta \ , \tag{4.16}$$

$$\hat{I}^{(j)}_{2,J}(.,k) = -\int_{\zeta=k\Delta x_3}^{x_3^{\mathrm{exit}}} \left\{ \prod_{\zeta'=\zeta}^{k\Delta x_3} \exp[-s\hat{\Gamma}^{(-)}(.,\zeta')\,\mathrm{d}\zeta'] \right\} \hat{X}^{(j)}_{2,J}(.,\zeta)\,\mathrm{d}\zeta \ , \tag{4.17}$$

with

$$\hat{X}^{(j)}_{1,2}(.,\zeta) = (\hat{R}\hat{W}^{(j-1)}_2)(.,\zeta) \ , \tag{4.18}$$

$$\hat{X}^{(j)}_{2,1}(.,\zeta) = (\hat{R}\hat{W}^{(j-1)}_1)(.,\zeta) \ , \tag{4.19}$$

$$\hat{X}^{(j)}_{2,2}(.,\zeta) = (\hat{T}\hat{W}^{(j-1)}_2)(.,\zeta) \ . \tag{4.20}$$

To construct the iteration scheme, we carry out the following steps. Let $\hat{P}$ denote the *thin-slab propagator*

$$\hat{P}(.,k) = \left\{ \prod_{\zeta'=(k-1)\Delta x_3}^{k\Delta x_3} \exp[-s\hat{\Gamma}^{(+)}(.,\zeta')\,\mathrm{d}\zeta'] \right\} \ . \tag{4.21}$$

We approximate the kernel of this propagator by Eq.(3.9) with $x_3' = (k-1)\Delta x_3$ and $x_3 = k\Delta x_3$. Then, using the semi-group property for the product integral,

$$\begin{aligned} \hat{I}^{(j)}_{1,1}(.,k) = & \left\{ \prod_{\zeta'=(k-1)\Delta x_3}^{k\Delta x_3} \exp[-s\hat{\Gamma}^{(+)}(.,\zeta')\,\mathrm{d}\zeta'] \right\} \\ & \int_{\zeta=0}^{(k-1)\Delta x_3} \left\{ \prod_{\zeta'=\zeta}^{(k-1)\Delta x_3} \exp[-s\hat{\Gamma}^{(+)}(.,\zeta')\,\mathrm{d}\zeta'] \right\} \hat{X}^{(j)}_{1,1}(.,\zeta)\,\mathrm{d}\zeta \\ & + \int_{\zeta=(k-1)\Delta x_3}^{k\Delta x_3} \left\{ \prod_{\zeta'=\zeta}^{k\Delta x_3} \exp[-s\hat{\Gamma}^{(+)}(.,\zeta')\,\mathrm{d}\zeta'] \right\} \hat{X}^{(j)}_{1,1}(.,\zeta)\,\mathrm{d}\zeta \ , \end{aligned} \tag{4.22}$$

which can be written as

$$\hat{I}^{(j)}_{1,1}(.,k) = \hat{P}(.,k)\,\hat{I}^{(j)}_{1,1}(.,k-1) + \hat{Q}^{(j)}_{1,1}(.,k)\ , \tag{4.23}$$

where

$$\hat{Q}^{(j)}_{1,1}(.,k) = \int_{\zeta=(k-1)\Delta x_3}^{k\Delta x_3} \left\{ \prod_{\zeta'=\zeta}^{k\Delta x_3} \exp[-s\hat{\Gamma}^{(+)}(.,\zeta')\,\mathrm{d}\zeta'] \right\} \hat{X}^{(j)}_{1,1}(.,\zeta)\,\mathrm{d}\zeta\ . \tag{4.24}$$

Recursion relations similar to the one in Eq.(4.23) can be found for the other elements of $\hat{I}$, viz.,

$$\begin{aligned} \hat{I}^{(j)}_{1,J}(.,k) &= \hat{P}(.,k)\,\hat{I}^{(j)}_{1,J}(.,k-1) + \hat{Q}^{(j)}_{1,J}(.,k) \quad \text{for} \quad k = 1,2,\cdots,M \quad , \\ \hat{I}^{(j)}_{2,J}(.,k) &= \hat{P}(.,k+1)\,\hat{I}^{(j)}_{2,J}(.,k+1) + \hat{Q}^{(j)}_{2,J}(.,k) \quad \text{for} \quad k = M-1,M-2,\cdots,0 \quad . \end{aligned} \tag{4.25}$$

Here

$$\hat{Q}^{(j)}_{1,J}(.,k) = \int_{\zeta=(k-1)\Delta x_3}^{k\Delta x_3} \left\{ \prod_{\zeta'=\zeta}^{k\Delta x_3} \exp[-s\hat{\Gamma}^{(+)}(.,\zeta')\,\mathrm{d}\zeta'] \right\} \hat{X}^{(j)}_{1,J}(.,\zeta)\,\mathrm{d}\zeta\ , \tag{4.26}$$

$$\hat{Q}^{(j)}_{2,J}(.,k) = \int_{\zeta=(k+1)\Delta x_3}^{k\Delta x_3} \left\{ \prod_{\zeta'=k\Delta x_3}^{\zeta} \exp[s\hat{\Gamma}^{(-)}(.,\zeta')\,\mathrm{d}\zeta'] \right\} \hat{X}^{(j)}_{2,J}(.,\zeta)\,\mathrm{d}\zeta\ . \tag{4.27}$$

Equations (4.25) describe a *marching* algorithm, the top one going forward and the bottom one going backward.

The initial values for the recursion scheme (4.25) are given by

$$\hat{I}^{(j)}_{1,J}(x_\mu,0) = 0\ , \tag{4.28}$$

$$\hat{I}^{(j)}_{2,J}(x_\mu,M) = 0\ , \tag{4.29}$$

again, for $j = 1,2,\cdots$.

Numerical issues

The implementation of the iterative scheme is as follows. It is initiated by the calculation of the incident field, $\hat{W}^{(0)}_1$, according to

$$\hat{W}^{(0)}_1(.,k\Delta x_3) = \hat{P}(.,k)\,\hat{W}^{(0)}_1(.,(k-1)\Delta x_3) \ \text{ for } \ k = 1,2,\cdots,M\ , \tag{4.30}$$

with initial condition

$$\hat{W}_1^{(0)}(.,0) = \hat{W}_1(.,0) \ , \tag{4.31}$$

according to Eq.(4.2). During the forward marching, at each of the discrete levels, $\hat{X}_{J,1}^{(1)}$ are computed and stored; $\hat{X}_{J,2}^{(1)}$ are set to zero. The procedure is continued by the backward propagation defined by the second iteration in Eq.(4.25). At each of the discrete levels, $\hat{W}_2^{(1)}$ is computed (Eq.(4.11)) and used to calculate $\hat{X}_{J,2}^{(2)}$; the latter quantity is stored as before. The scheme continues to switch from backward to forward propagation based on the first iteration in Eq.(4.25), and so on.

To evaluate the elements of $\hat{Q}^{(j)}$, we apply the trapezoidal rule. Then

$$\hat{Q}_{1,J}^{(j)}(.,k) \simeq \ \tfrac{1}{2}\Delta x_3 \left[\hat{X}_{1,J}^{(j)}(.,k\Delta x_3) + \hat{P}(.,k)\, \hat{X}_{1,J}^{(j)}(.,(k-1)\Delta x_3)\right] \ , \tag{4.32}$$

$$\hat{Q}_{2,J}^{(j)}(.,k) \simeq -\tfrac{1}{2}\Delta x_3 \left[\hat{X}_{2,J}^{(j)}(.,k\Delta x_3) + \hat{P}(.,k+1)\, \hat{X}_{2,J}^{(j)}(.,(k+1)\Delta x_3)\right] \ . \tag{4.33}$$

which formulas are accurate $\mathcal{O}((\Delta x_3)^2)$.

In the remainder of this paper, we will derive approximate, screen representations for $\hat{\Gamma}$, $\hat{P}$, $\hat{\Gamma}^{-1}$ and $\hat{R}$. This will lead to an overal multiple screen representation of the full solution of the acoustic wave equation.

5 Screen representation of the propagator

There exists a wide variety of techniques to approximate the vertical slowness symbol to speed up the computation of the one-sided propagator Eq.(3.8) generated by Eq.(3.9). Here, we pursue the perturbative, split-step Fourier approach (Stoffa *et al.* [12]) to arrive at a generalized-screen expansion of the propagator. A schematic view of this expansion is shown in Figure 5.1 (the symbols will be explained in the later analysis). Underlying the generalized-screen approach is an embedding procedure.

To introduce the embedding, consider a thin slab, $[x_3', x_3]$, with thickness $\Delta x_3 = x_3 - x_3'$. We introduce a *background* medium in the slab, with parameters ρ^0, κ^0. The background medium, or embedding, is constant in the slab, but may vary from one slab to another:

$$\rho^0(\zeta) = \rho^0(x_3) \ , \quad \kappa^0(\zeta) = \kappa^0(x_3) \ , \quad \zeta \in [x_3', x_3] \ .$$

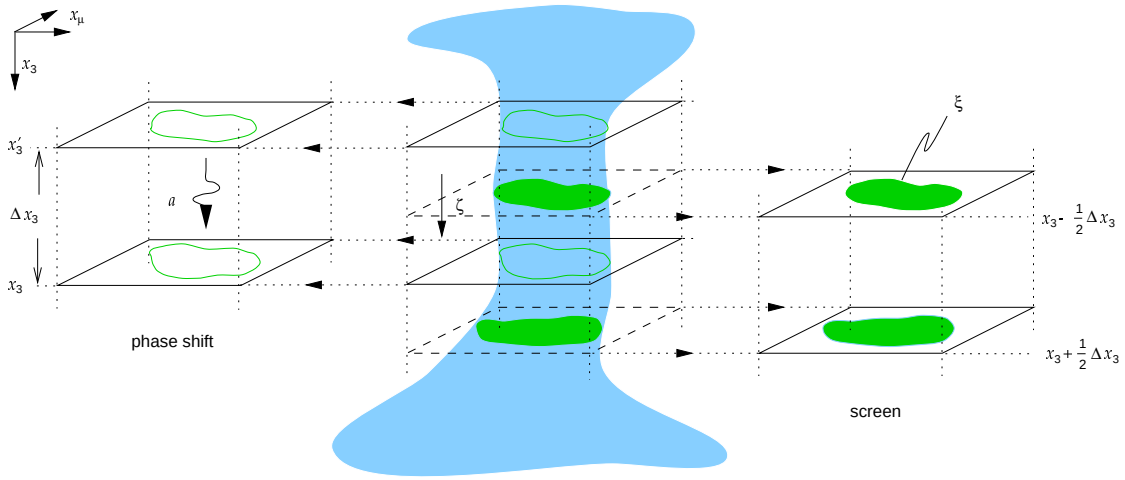

Figure 5.1: The screen representation for one-way propagation.

The vertical slowness left symbol, contrast formulation

In the acoustic pressure normalization analog, the characteristic differential operator in Eq.(2.18) is given by

$$\hat{\mathrm{A}} = -D_\nu D_\nu + \kappa\rho - \rho^{-1}(D_\nu\rho)\, D_\nu - \rho^{-1}(D_\nu^2\rho) + \rho^{-2}(D_\nu\rho)^2 \ , \tag{5.1}$$

with left symbol $\hat{\mathrm{a}} = \hat{\mathrm{a}}(x_\mu, \zeta, \alpha_\nu)$. For the further analysis, we will employ a *contrast* formulation. Having introduced in the interval $[x_3', x_3]$ a background medium with parameters ρ^0, κ^0, the medium perturbation is given by

$$\epsilon_\kappa(x_\mu,\zeta) = \frac{\kappa^0(x_3)}{\kappa(x_\mu,\zeta)} - 1 \quad , \quad \epsilon_\rho(x_\mu,\zeta) = \frac{\rho(x_\mu,\zeta)}{\rho^0(x_3)} - 1 \ ; \tag{5.2}$$

$$c = (\kappa\rho)^{-1/2} \quad , \quad c^0 = (\kappa^0\rho^0)^{-1/2} \ , \tag{5.3}$$

for $\zeta \in [x_3', x_3]$.

We will now expand the left symbol $\hat{\mathrm{a}}$ of $\hat{\mathrm{A}}$ simultaneously in medium contrast (the order is indicated by a superscript) and in symbol (or operator) order (this order is indicated by a subscript). Thus, expanding $\hat{\mathrm{a}}$ in medium contrast, yields the decomposition $\hat{\mathrm{a}} = \hat{\mathrm{a}}^0 + \hat{\mathrm{a}}^1 + \hat{\mathrm{a}}^2$, while expanding the individual terms appearing in the decomposition further into symbol order, leads to

$$\hat{\mathrm{a}}^0 \ = \ \hat{\mathrm{a}}^0_2 = \alpha_\nu^2 + (c^0)^{-2} \tag{5.4}$$

for the background, and

$$\hat{\mathrm{a}}^1 \;=\; \hat{\mathrm{a}}^1_2 + \hat{\mathrm{a}}^1_1 + \hat{\mathrm{a}}^1_0 \;, \tag{5.5}$$

and

$$\hat{\mathrm{a}}^2 \;=\; \hat{\mathrm{a}}^2_0 = (\rho^0)^2\rho^{-2}(D_\nu\epsilon_\rho)^2 \tag{5.6}$$

for the contrast. Here,

$$\begin{aligned}
\hat{\mathrm{a}}^1_2 &= \quad (c^0)^{-2}\epsilon_\rho - c^{-2}\epsilon_\kappa \quad , \\
\hat{\mathrm{a}}^1_1 &= -\rho^0\rho^{-1}(D_\nu\epsilon_\rho)\,\mathrm{i}\alpha_\nu \quad , \\
\hat{\mathrm{a}}^1_0 &= -\rho^0\rho^{-1}(D^2_\nu\epsilon_\rho) \qquad .
\end{aligned} \tag{5.7}$$

Given the symbol $\hat{\mathrm{a}}$, we now have to construct the vertical slowness left symbol $\hat{\gamma}^{(\pm)}$ defined in Eq.(3.7). This symbol satisfies a characteristic equation following the composition of operators in Eq.(2.18) [1]:

$$\exp\left[-\mathrm{i}\,\partial_{\alpha'_\sigma}D_{x'_\sigma}\right]\,\hat{\gamma}(x_\mu,\zeta,\alpha'_\sigma)\hat{\gamma}(x'_\sigma,\zeta,\alpha_\nu)\,\Big|_{(x'_\mu,\alpha'_\nu)=(x_\mu,\alpha_\nu)} = \hat{\mathrm{a}}(x_\mu,\zeta,\alpha_\nu)\;. \tag{5.8}$$

(The composition equation for the associated Weyl symbols follows from the work of Fishman and McCoy [11]). This equation defines the generalized slowness surface and has solutions $\hat{\gamma}^{(\pm)}$. The two branches are $\hat{\gamma}^{(\pm)}(x_\mu,\zeta,\alpha_\nu)$ such that $\mathrm{Re}\{\hat{\gamma}^{(+)}(x_\mu,\zeta,\alpha_\nu)\} \geq 0$ and $\mathrm{Re}\{\hat{\gamma}^{(-)}(x_\mu,\zeta,\alpha_\nu)\} \leq 0$. Due to the local up/down symmetry of the medium we have $\hat{\gamma}^{(+)} = -\hat{\gamma}^{(-)}$. Note that as $s \to \infty$ the composition of symbols tends to an ordinary multiplication, and the solution of Eq.(5.8) reduces to the principal parts of the symbols. The principal part of the vertical slowness symbol corresponds to the vertical gradient of travel time, in accordance with the eikonal equation (which can be obtained from the high-frequency approximation of the path integral, see De Hoop [1]).

Scaling

The solution, $\hat{\gamma}$, to Eq.(5.8) will be constructed by means of a (polyhomogeneous) series expansion following the expansion of $\hat{\mathrm{a}}$ introduced above. To ease the identification of medium-contrast and symbol orders in the construction, we introduce two dimensionless parameters, ε associated with the medium constrast and Ω associated with the symbol order. With these

parameters, we control the *magnitude* of our medium contrast (ε) and the *smoothness* (Ω) also, i.e.

$$\epsilon_\kappa(x_\mu,\zeta) = \varepsilon\, \mathsf{e}_\kappa(\Omega x_\mu,\zeta)\ , \qquad \epsilon_\rho(x_\mu,\zeta) = \varepsilon\, \mathsf{e}_\rho(\Omega x_\mu,\zeta)\ . \tag{5.9}$$

With

$$\begin{aligned} \rho^0\rho^{-1} &= 1-\varepsilon\,\mathsf{e}_\rho+\varepsilon^2\,\mathsf{e}_\rho^2 &&, \\ (\rho^0)^2\rho^{-2} &= 1-2\varepsilon\,\mathsf{e}_\rho+3\varepsilon^2\,\mathsf{e}_\rho^2 &&, \\ (\kappa^0)^{-1}\kappa &= 1-\varepsilon\,\mathsf{e}_\kappa+\varepsilon^2\,\mathsf{e}_\kappa^2 &&, \\ (c^0)^2c^{-2} &= 1+\varepsilon\,(\mathsf{e}_\rho-\mathsf{e}_\kappa)-\varepsilon^2\,\mathsf{e}_\kappa\,(\mathsf{e}_\rho-\mathsf{e}_\kappa) &&, \end{aligned} \tag{5.10}$$

up to $\mathcal{O}(\varepsilon^2)$, we rewrite the expansion of the symbol $\hat{\mathrm{a}}$ associated with the characteristic operator as (cf. Eq.(5.7))

$$\begin{aligned} \hat{\mathrm{a}}_2^1 &= \varepsilon(c^0)^{-2}\{\mathsf{e}_\rho-\mathsf{e}_\kappa[1+\varepsilon\,(\mathsf{e}_\rho-\mathsf{e}_\kappa)-\varepsilon^2\,\mathsf{e}_\kappa(\mathsf{e}_\rho-\mathsf{e}_\kappa)+\cdots]\} &&, \\ \hat{\mathrm{a}}_1^1 &= -\varepsilon\Omega\ \{1-\varepsilon\,\mathsf{e}_\rho+\varepsilon^2\,\mathsf{e}_\rho^2+\cdots\}\,(\mathsf{D}_\nu\mathsf{e}_\rho)\,\mathrm{i}\alpha_\nu &&, \\ \hat{\mathrm{a}}_0^1 &= -\varepsilon\Omega^2\{1-\varepsilon\,\mathsf{e}_\rho+\varepsilon^2\,\mathsf{e}_\rho^2+\cdots\}\,(\mathsf{D}_\nu^2\mathsf{e}_\rho) &&, \end{aligned} \tag{5.11}$$

while (cf. Eq.(5.6))

$$\hat{\mathrm{a}}_0^2 = \varepsilon^2\Omega^2\,\{1-2\varepsilon\,\mathsf{e}_\rho+\cdots\}\,(\mathsf{D}_\nu\mathsf{e}_\rho)^2\ . \tag{5.12}$$

We have introduced the scaled horizontal slowness operators D_ν which differentiates with respect to Ωx_ν: $\mathsf{D}_\nu = \Omega^{-1}D_\nu$. The expansions shown above appear in the Born series also (see Appendix A), which occurs naturally in the parameters ρ and κ. Here, we will treat the expansions in Eqs.(5.11)-(5.12) between braces as single expressions and thus reparametrize the series for the characteristic symbol.

The symbol $\hat{\mathrm{a}}_2^1$ is directly related to the *screen* function $S_{c^{-1}}$ [13] which we will encounter in the later analysis. Let $\epsilon_{c^{-1}}(x_\mu,\zeta)$ denote the relative medium slowness perturbation for $\zeta\in[x_3',x_3]$, then

$$\tfrac{1}{2}\hat{\mathrm{a}}_2^1 \simeq (c^0)^{-2}\,\epsilon_{c^{-1}}\ , \quad \epsilon_{c^{-1}} \simeq \tfrac{1}{2}(\mathsf{e}_\rho-\mathsf{e}_\kappa)\ , \quad \text{while} \quad S_{c^{-1}} = \frac{1}{\Delta x_3}\int_{x_3'}^{x_3}\epsilon_{c^{-1}}\,\mathrm{d}\zeta\ . \tag{5.13}$$

These approximations are $\mathcal{O}(\varepsilon^2)$.

Perturbation expansion of the vertical slowness left symbol

We will solve Eq.(5.8) by method of expansion. In view of the contrast formulation, the vertical slowness in the laterally homogeneous embedding is introduced (cf. Eq.(5.4))

$$\gamma^0(\zeta,\alpha_\nu,s)=\sqrt{\hat{\mathrm{a}}_2^0(x_3,\alpha_\nu)}=\sqrt{\alpha_\nu^2+[c^0(x_3)]^{-2}}=\gamma^0(x_3,\alpha_\nu)\ \text{ if }\ \zeta\in[x_3',x_3]\ . \tag{5.14}$$

We suppose that the vertical slowness symbol can be appoximated by a perturbation, $\hat{\gamma}^1$ say, superimposed on the vertical slowness in the laterally homogeneous embedding,

$$\hat{\gamma}(x_\mu,\zeta,\alpha_\nu,s)=\gamma^0(x_3,\alpha_\nu)+\hat{\gamma}^1(x_\mu,\zeta,\alpha_\nu,s)\ \text{ if }\ \zeta\in[x_3',x_3]\ . \tag{5.15}$$

First, let us expand the vertical slowness perturbation, asymptotically into the magnitude of the medium perturbation, i.e.

$$\hat{\gamma}^1(x_\mu,\zeta,\alpha_\nu,s)\sim\sum_{n=1}^{\infty}\varepsilon^n\,\eta^{[n]}(x_\mu,\zeta,\alpha_\nu,s)\ ; \tag{5.16}$$

this expansion, though carried out in the space of symbols, has similarities with the Born series expansion (see, e.g., A.T. de Hoop [33]). Associated with the Born approximation is the condition

$$c(x_\mu,\zeta)\geq c^0(x_3)\ , \tag{5.17}$$

which for the symbols guarantees that no artificial branch point will enter the propagating-wave domain. Also, note that this expansion breaks down where the exact symbol fails to be analytic.

Second, we expand the series (5.16) further in terms of the smoothness of the medium perturbation,

$$\eta^{[n]}(x_\mu,\zeta,\alpha_\nu,s)\sim\sum_{m=0}^{\infty}\Omega^m\,\eta^{[n]}_{[1-m]}(x_\mu,\zeta,\alpha_\nu,s)\ . \tag{5.18}$$

The leading term of this expansion represents the high-frequency approximation or the principal part. We will suppress the dependencies on ζ and s in our notation.

While substituting these expansions into Eq.(5.8), we observe that for $k\geq 1$,

$$(-\mathrm{i}\partial_{\alpha_\sigma'}D_{x_\sigma'})^k\hat{\gamma}(x_\mu,\alpha_\sigma')\hat{\gamma}(x_\sigma',\alpha_\nu)\Big|_{(x_\mu',\alpha_\nu')=(x_\mu,\alpha_\nu)}= \tag{5.19}$$

$$\sum_{\ell=0}^{k}\left(\begin{array}{c}k\\ \ell\end{array}\right)(-\mathrm{i})^k[(\partial_{\alpha_1}^{k-\ell}\partial_{\alpha_2}^{\ell}\gamma^0)(x_\mu,\alpha_\nu)+(\partial_{\alpha_1}^{k-\ell}\partial_{\alpha_2}^{\ell}\hat{\gamma}^1)(x_\mu,\alpha_\nu)]\,(D_{x_1}^{k-\ell}D_{x_2}^{\ell}\hat{\gamma}^1)(x_\mu,\alpha_\nu)\ ,$$

hence

$$(-\mathrm{i}\partial_{\alpha'_\sigma} D_{x'_\sigma})^k \hat{\gamma}(x_\mu, \alpha'_\sigma)\hat{\gamma}(x'_\sigma, \alpha_\nu)\Big|_{(x'_\mu,\alpha'_\nu)=(x_\mu,\alpha_\nu)} = \sum_{\ell=0}^{k} \left(\begin{array}{c} k \\ \ell \end{array} \right) (-\mathrm{i})^k \Omega^k \sum_{n'=1}^{\infty} \varepsilon^{n'} \sum_{m'=0}^{\infty} \Omega^{m'}$$

$$\left[(\partial_{\alpha_1}^{k-\ell}\partial_{\alpha_2}^{\ell}\gamma^0)(x_\mu,\alpha_\nu) + \sum_{n=1}^{\infty} \varepsilon^n \sum_{m=0}^{\infty} \Omega^m \, (\partial_{\alpha_1}^{k-\ell}\partial_{\alpha_2}^{\ell}\eta^{[n]}_{[1-m]})(x_\mu,\alpha_\nu) \right] \, (\mathsf{D}_{x_1}^{k-\ell}\mathsf{D}_{x_2}^{\ell}\eta^{[n']}_{[1-m']})(x_\mu,\alpha_\nu) \; . \tag{5.20}$$

Upon substituting the expansions (5.16)-(5.18) into Eq.(5.8), we will collect terms of equal order in ε. These terms are then separated in orders of Ω. We will carry out our analysis up to $\mathcal{O}(\Omega^2)$.

The terms $\mathcal{O}(\varepsilon^0)$ yield Eq.(5.14), viz.

$$(\gamma^0)^2 = \hat{\mathrm{a}}_2^0 \qquad [k=0] \tag{5.21}$$

which is $\mathcal{O}(\Omega^0)$. The terms $\mathcal{O}(\varepsilon)$ decompose into

$$2\gamma^0 \, \eta^{[1]}_{[1]} = \hat{\mathrm{a}}_2^1 \qquad [k=0] \tag{5.22}$$

which is $\mathcal{O}(\Omega^0)$, and

$$2\gamma^0 \, \eta^{[1]}_{[1-m]} - \mathrm{i}\,(\partial_{\alpha_\sigma}\gamma^0)\,(\mathsf{D}_{x_\sigma}\eta^{[1]}_{[1-(m-1)]}) = \hat{\mathrm{a}}^1_{2-m} \; , \qquad m=1,2 \qquad [k=0,1] \tag{5.23}$$

which is $\mathcal{O}(\Omega^m)$. The terms $\mathcal{O}(\varepsilon^2)$ decompose into

$$(\eta^{[1]}_{[1]})^2 + 2\gamma^0 \, \eta^{[2]}_{[1]} = 0 \qquad [k=0] \tag{5.24}$$

which is $\mathcal{O}(\Omega^0)$,

$$2\eta^{[1]}_{[1]}\eta^{[1]}_{[0]} + 2\gamma^0 \, \eta^{[2]}_{[0]} - \mathrm{i}\,(\partial_{\alpha_\sigma}\gamma^0)\,(\mathsf{D}_{x_\sigma}\eta^{[2]}_{[1]}) - \mathrm{i}\,(\partial_{\alpha_\sigma}\eta^{[1]}_{[1]})\,(\mathsf{D}_{x_\sigma}\eta^{[1]}_{[1]}) = 0 \qquad [k=0,1] \tag{5.25}$$

which is $\mathcal{O}(\Omega)$, and

$$\begin{aligned} & 2\gamma^0 \, \eta^{[2]}_{[-1]} + (\eta^{[1]}_{[0]})^2 + 2\eta^{[1]}_{[1]}\eta^{[1]}_{[-1]} && [k=0] \\ & - \mathrm{i}\,[(\partial_{\alpha_\sigma}\gamma^0)\,(\mathsf{D}_{x_\sigma}\eta^{[2]}_{[0]}) + (\partial_{\alpha_\sigma}\eta^{[1]}_{[1]})\,(\mathsf{D}_{x_\sigma}\eta^{[1]}_{[0]}) + (\partial_{\alpha_\sigma}\eta^{[1]}_{[0]})\,(\mathsf{D}_{x_\sigma}\eta^{[1]}_{[1]})] && [k=1] \\ & - \tfrac{1}{2}[(\partial^2_{\alpha_1}\gamma^0)(\mathsf{D}^2_{x_1}\eta^{[2]}_{[1]}) + 2(\partial_{\alpha_1}\partial_{\alpha_2}\gamma^0)(\mathsf{D}_{x_1}\mathsf{D}_{x_2}\eta^{[2]}_{[1]}) + (\partial^2_{\alpha_2}\gamma^0)(\mathsf{D}^2_{x_2}\eta^{[2]}_{[1]}) && [k=2] \\ & \quad + (\partial^2_{\alpha_1}\eta^{[1]}_{[1]})(\mathsf{D}^2_{x_1}\eta^{[1]}_{[1]}) + 2(\partial_{\alpha_1}\partial_{\alpha_2}\eta^{[1]}_{[1]})(\mathsf{D}_{x_1}\mathsf{D}_{x_2}\eta^{[1]}_{[1]}) + (\partial^2_{\alpha_2}\eta^{[1]}_{[1]})(\mathsf{D}^2_{x_2}\eta^{[1]}_{[1]})] && [k=2] \\ & = \hat{\mathrm{a}}^2_0 \end{aligned} \tag{5.26}$$

which is $\mathcal{O}(\Omega^2)$. Etc.

Solving the equations $\mathcal{O}(\Omega^0)$, i.e. for $\eta^{[n]}_{[1]}$, we observe that the constituent symbols generate an expansion of the type

$$\hat{\gamma}_1 = \sqrt{\hat{\mathrm{a}}^0_2 + \hat{\mathrm{a}}^1_2} = \gamma^0 \sqrt{1 + (\hat{\mathrm{a}}^1_2/\hat{\mathrm{a}}^0_2)} \sim \gamma^0 + \sum_{n=1}^{\infty} \varepsilon^n \, \eta^{[n]}_{[1]} \, , \tag{5.27}$$

which could also be rewritten as

$$\sqrt{\hat{\mathrm{a}}^0_2 + \hat{\mathrm{a}}^1_2} = \sqrt{\hat{\mathrm{a}}^1_2} \sqrt{1 + (\hat{\mathrm{a}}^0_2/\hat{\mathrm{a}}^1_2)}$$

and expanded in a Taylor series accordingly. The first three terms of expansion (5.27) are illustrated in Figure 5.2. In this figure, we have carried out the rotations in the frequency and slowness domains

$$s = \mathrm{i}\omega \, , \quad \alpha_\nu = -\mathrm{i}p_\nu \, .$$

Solving the equations $\mathcal{O}(\Omega)$, i.e. for $\eta^{[n]}_{[0]}$, we find that the constituent symbols represent an expansion of the type [1, Section VIII]

$$\frac{1}{2\,[\hat{\mathrm{a}}^0_2 + \hat{\mathrm{a}}^1_2]^{3/2}} \left[\hat{\mathrm{a}}^1_1\,[\hat{\mathrm{a}}^0_2 + \hat{\mathrm{a}}^1_2] + \tfrac{1}{2}\mathrm{i}\alpha_\sigma (D_{x_\sigma} \hat{\mathrm{a}}^1_2)\right] \tag{5.28}$$

$$= \frac{1}{2(\gamma^0)^3\,[1 + (\hat{\mathrm{a}}^1_2/\hat{\mathrm{a}}^0_2)]^{3/2}} \left[(\gamma^0)^2 \hat{\mathrm{a}}^1_1\,[1 + (\hat{\mathrm{a}}^1_2/\hat{\mathrm{a}}^0_2)] + \tfrac{1}{2}\mathrm{i}\alpha_\sigma (D_{x_\sigma} \hat{\mathrm{a}}^1_2)\right] \sim \sum_{n=1}^{\infty} \varepsilon^n \, \eta^{[n]}_{[0]} \, ,$$

which takes into account the rate of change (gradient) of the medium properties in the lateral directions.

Screen reduction

The recursion for the solution of the vertical slowness left symbol described by Eqs.(5.21)-(5.26) reveals that the expansion in ε implies a separation in the phase space coordinates, x_μ and α_ν, of the constituent symbols in Eq.(5.18):

$$\eta^{[n]}_{[1-m]}(x_\mu, \alpha_\nu) = \sum_{\lambda} \overset{\lambda}{\xi}{}^{[n]}_{[1-m]} \, (x_\mu) \; \overset{\lambda}{a}{}^{[n]}_{[1-m]} \, (\alpha_\nu) \, , \quad m = 0, 1, \cdots \tag{5.29}$$

We will illustrate the implications of this expansion for the case $n = 1$ and $m = 0$, when we have one term only. To simplify the notation, in this case, we omit the counter λ. Representation (5.29) is depicted in Figure 5.1.

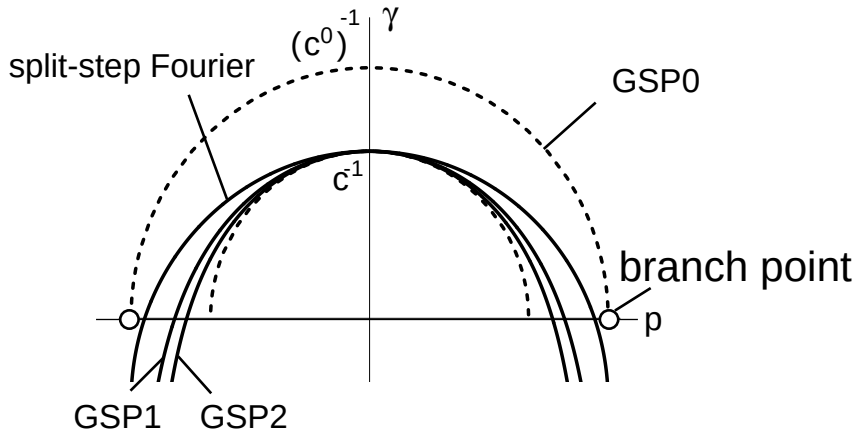

Figure 5.2: Principal parts of the generalized screen vertical slowness left symbols: zero order (GSP0), first order (GSP1) and second order (GSP2). 'Split-step' refers to the phase screen.

The separation of variables is why our lattice integral Eq.(3.8) will reduce to a screen propagator [13]. Equation (5.29) implies the following structure for the *cokernel* (cf. Eq.(3.13)) of the vertical slowness operator,

$$\widetilde{\eta^{[n]}_{[1-m]}}(\alpha_\mu - \alpha''_\mu, \alpha''_\nu) = \widetilde{\xi^{[n]}_{[1-m]}}(\alpha_\mu - \alpha''_\mu)\, a^{[n]}_{[1-m]}(\alpha''_\nu)\ , \quad m = 0, 1, \cdots \tag{5.30}$$

which reveals how Fourier constituents ('plane' waves) interact. Asymptotically, we have

$$\widetilde{\xi^{[n]}_{[1-m]}}(\alpha_\mu - \alpha''_\mu) \sim s^{-2}\ \left\{\xi^{[n]}_{[1-m]}(0)\,\delta(\alpha_\mu - \alpha''_\mu) + \mathrm{i}\Omega\,(\mathsf{D}_{x_\sigma}\xi^{[n]}_{[1-m]})(0)\,(\partial_{\alpha_\sigma}\delta)(\alpha_\mu - \alpha''_\mu) + \cdots\right\}\ .$$

Let us consider the expansion for the vertical slowness left symbol up to $\mathcal{O}(\varepsilon)$ and $\mathcal{O}(\Omega^0)$. Using Eq.(5.27), we arrive at

$$\eta^{[1]}_{[1]}(x_\mu, \alpha_\nu) = \xi^{[1]}_{[1]}(x_\mu)\, a^{[1]}_{[1]}(\alpha_\nu)\ , \qquad \xi^{[1]}_{[1]} = \tfrac{1}{2}\hat{\mathsf{a}}^1_2\ , \quad a^{[1]}_{[1]} = \frac{1}{\gamma^0}\ . \tag{5.31}$$

We denote this first-order expansion as the *wide-angle screen* approximation. (How the wide-angle screen approximation relates to the local-Born approximation is discussed in Appendix A.) Observe the occurrence of the branch point associated with the background medium, which is artificial. Ignoring the artifial branch point, we now Taylor expand the factor $a^{[1]}_{[1]}$ about $\alpha_\nu = 0$ (limiting to narrow angles). Up to zero-order,

$$a^{[1]}_{[1]}(\alpha_\nu) \simeq a^{[1]}_{[1]}(0) = c^0\ , \tag{5.32}$$

which leads to the *phase-screen* or split-step approximation, which is also shown in Figure 5.2. For various applications, the second-order expansion in α_ν^2 is sufficiently accurate,

$$a_{[1]}^{[1]}(\alpha_\nu) \simeq c^0 - \tfrac{1}{2}(c^0)^3\ \alpha_\nu^2 + \tfrac{3}{8}(c^0)^5\ (\alpha_\nu^2)^2\ . \tag{5.33}$$

These expansions are illustrated in Figure 5.3. Note that, upon carrying out the Taylor expansion of $a_{[1]}^{[1]}$ in α_ν, we can replace the background from *minimum* value in the thin slab to *average* value, thus enhancing the accuracy [12]. This replacement also represents the transition from the phase-screen to the split-step Fourier approach. Some wavefronts associated with Figures 5.2 and 5.3 are shown in Figure 5.4. Using Huygens principle, we can now anticipate the evolution of a wavefront in a heterogeneous medium. In all the approximations, independent of order, the propagation speed in the horizontal directions is c^0, which causes any of our approximate instantaneous wavefronts to fold inwards away from the true instantaneous wavefront. As such, the generalized-screen approximation differs, for example, from the paraxial approximation where the accuracy with propagation angle is *independent* of the medium [5, 7]. But, like in the paraxial approximation, *critical-angle* phenomena are *not* modelled properly within the generalized-screen approximation.

The contribution to the left symbol $\mathcal{O}(\varepsilon)$ and $\mathcal{O}(\Omega)$ follows directly from Eq.(5.23) as

$$\eta_{[0]}^{[1]} = \tfrac{1}{2}\hat{\mathrm{a}}_1^1\,\frac{1}{\gamma^0} + \tfrac{1}{4}(D_{x_\sigma}\hat{\mathrm{a}}_2^1)\,\frac{\mathrm{i}\alpha_\sigma}{(\gamma^0)^3}\ , \tag{5.34}$$

which extends the wide-angle approximation Eq.(5.31).

Optimization

Rather than accepting a given order of expansion, we will discuss a way – introducing intermediate parameters – to smear out the error of our approximation in phase space. In particular, we will be concerned about the errors in travel times along the wave-constituent characteristics, and try to minimize those. Such errors are associated with the principal parts of the symbols.

As an example, consider the wide-angle approximation (5.31). By shifting the background medium branch points in this expression, we can 'bend' the principal part of the slowness curve. We will exploit this bending in an optimization procedure. In Eqs.(5.15) and (5.31), we introduce parameters β_0, β_1 according to

$$\gamma^0(x_3,\alpha_\nu) \to \sqrt{\beta_0\alpha_\nu^2 + [c^0(x_3)]^{-2}}\ , \qquad a_{[1]}^{[1]}(\alpha_\nu) \to \frac{1}{\sqrt{\beta_1\alpha_\nu^2 + [c^0(x_3)]^{-2}}}\ . \tag{5.35}$$

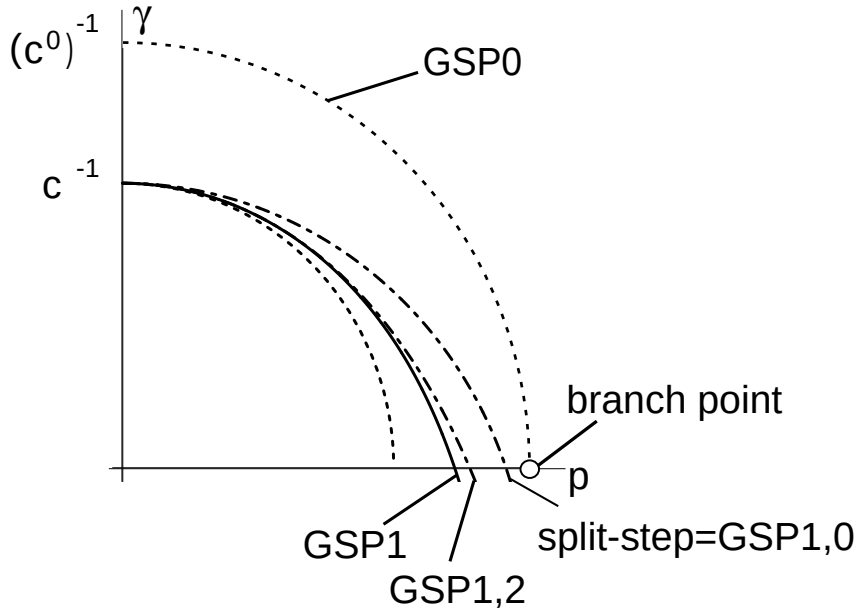

Figure 5.3: Taylor expansions of the principal part of the first-order generalized screen (GSP1) vertical slowness left symbol: zero order (GSP1,0) and second order (GSP1,2).

If the range of scattering angles is limited, by adjusting β_0, β_1, indeed the branch points can be moved inwards. However, upon applying the Taylor series expansion (5.33), the troublesome branch point in $a^{[1]}_{[1]}$ is removed; then we set

$$\gamma^0(x_3,\alpha_\nu) \to \gamma^0(x_3,\alpha_\nu)\ , \qquad a^{[1]}_{[1]}(\alpha_\nu) \to c^0 - \tfrac{1}{2}(c^0)^3\ \beta_0\alpha_\nu^2 + \tfrac{3}{8}(c^0)^5\ \beta_1(\alpha_\nu^2)^2 \tag{5.36}$$

instead.

For the purpose of optimization, we will turn the composition equation (5.8) into a weak form, viz., we introduce the error function

$$\mathrm{err}(x_\mu,\zeta,s) = (s/2\pi)^2 \int \tag{5.37}$$

$$\left|\exp\left[-\mathrm{i}\,\partial_{\alpha'_\sigma} D_{x'_\sigma}\right]\ \hat\gamma(x_\mu,\zeta,\alpha'_\sigma,s)\hat\gamma(x'_\sigma,\zeta,\alpha_\nu,s)\,\Big|_{(x'_\mu,\alpha'_\nu)=(x_\mu,\alpha_\nu)} - \hat{\mathrm{a}}(x_\mu,\zeta,\alpha_\nu,s)\right|^2 \mathrm{d}\alpha_1\mathrm{d}\alpha_2\ ,$$

measuring an L^2 average over the horizontal slownesses up to the branch points (i.e., over the 'propagating' slowness surface). Restricting the error function to $\mathcal{O}(\Omega^0)$, i.e. the vertical gradients of travel time, yields

$$\mathrm{err}^{[N]}_{[1]}(x_\mu,\zeta;\beta) = (s/2\pi)^2 \int \tag{5.38}$$

$$\left|\left[\gamma^0(x_3,\alpha_\nu) + \sum_{n=1}^{N}\varepsilon^n\,\eta^{[n]}_{[1]}(x_\mu,\zeta,\alpha_\nu)\right]^2 - \hat{\mathrm{a}}^0_2(x_\mu,\zeta,\alpha_\nu)\right|^2 \mathrm{d}\alpha_1\mathrm{d}\alpha_2\ .$$

The misfit in the optimization for parameters β_0, β_1 is then simply the integral of the error function over horizontal space. This integration reflects the variation of the medium in the horizontal directions. Thus, for the $\mathcal{O}(\Omega^0)$ optimization problem, we might integrate over the associated range of medium slownesses instead.

Enforcing the parameters β_0, β_1 to be equal ensures that the approximate expression (5.35) contains a single branch point only. To ensure that the approximate expression reduces to a screen representation, the parameters should be independent of x_μ.

The screen propagator

We will now return to the basic symbol structure Eqs.(5.15),(5.31) and analyze what this structure implies for the thin-slab propagator given in Eq.(3.9). In general, with Eq.(5.15) we get

$$\hat g^{(+)}(x_\mu,x_3;x'_\nu,x_3-\Delta x_3) \simeq \int (s/2\pi)^2 \mathrm{d}\alpha''_1\mathrm{d}\alpha''_2 \tag{5.39}$$

$$\exp[-\mathrm{i}s\,\alpha''_\sigma(x_\sigma - x'_\sigma)]\ \exp[-s\,\{\gamma^0(x_3-\Delta x_3,\alpha''_\nu) + \hat\gamma^1(x_\mu, x_3-\tfrac{1}{2}\Delta x_3,\alpha''_\nu)\}\,\Delta x_3]\ .$$

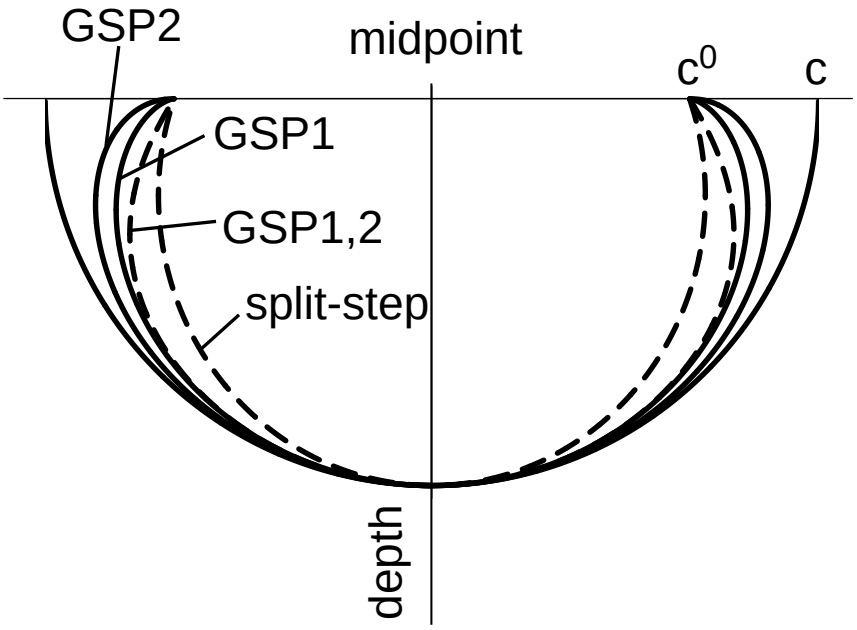

Figure 5.4: Wavefronts associated with the various generalized-screen approximations.

Invoking the first-order generalized-screen approximation (5.31) yields

$$\exp[-s\,\{\gamma^0(x_3-\Delta x_3,\alpha_\nu'')+\hat\gamma^1(x_\mu,x_3-\tfrac{1}{2}\Delta x_3,\alpha_\nu'')\}\,\Delta x_3] \tag{5.40}$$

$$\simeq \exp[-s\varepsilon\,\xi^{[1]}_{[1]}(x_\mu,x_3-\tfrac{1}{2}\Delta x_3)a^{[1]}_{[1]}(x_3-\tfrac{1}{2}\Delta x_3,0)\;\Delta x_3]\;\exp[-s\,\gamma^0(x_3-\Delta x_3,\alpha_\nu'')\,\Delta x_3]$$

$$\exp[-s\varepsilon\,\xi^{[1]}_{[1]}(x_\mu,x_3-\tfrac{1}{2}\Delta x_3)\,[a^{[1]}_{[1]}(x_3-\tfrac{1}{2}\Delta x_3,\alpha_\nu'')-a^{[1]}_{[1]}(x_3-\tfrac{1}{2}\Delta x_3,0)]\;\Delta x_3]$$

$$\simeq \exp[-s\varepsilon\,\xi^{[1]}_{[1]}(x_\mu,x_3-\tfrac{1}{2}\Delta x_3)a^{[1]}_{[1]}(x_3-\tfrac{1}{2}\Delta x_3,0)\;\Delta x_3]\;\exp[-s\,\gamma^0(x_3-\Delta x_3,\alpha_\nu'')\,\Delta x_3]$$

$$\left\{1-s\varepsilon\,\xi^{[1]}_{[1]}(x_\mu,x_3-\tfrac{1}{2}\Delta x_3)\,[a^{[1]}_{[1]}(x_3-\tfrac{1}{2}\Delta x_3,\alpha_\nu'')-a^{[1]}_{[1]}(x_3-\tfrac{1}{2}\Delta x_3,0)]\;\Delta x_3\right\}$$

if

$$\frac{s\,\Delta x_3}{c^0}\;\left|\varepsilon\,c^0\xi^{[1]}_{[1]}(x_\mu,.)\,[a^{[1]}_{[1]}(.,\alpha_\nu'')-a^{[1]}_{[1]}(.,0)]\right|\ll 1\;.$$

Note that $\varepsilon\,c^0\xi^{[1]}_{[1]}=(c^0)^{-1}S_{c^{-1}}$ represents the absolute medium slowness perturbation, while $[a^{[1]}_{[1]}(.,\alpha_\nu'')-a^{[1]}_{[1]}(.,0)]$ vanishes at normal incidence ($\alpha_\nu''=0$) and is bounded by c^0 as $\alpha_\nu''\alpha_\nu''\to\infty$.

Substituting Eq.(5.40) into Eq.(5.39) results in

$$\hat{g}^{(+)}(x_\mu, x_3; x'_\nu, x_3 - \Delta x_3) \simeq \exp[-s\varepsilon\, \xi^{[1]}_{[1]}(x_\mu, x_3 - \tfrac{1}{2}\Delta x_3) a^{[1]}_{[1]}(x_3 - \tfrac{1}{2}\Delta x_3, 0)\ \Delta x_3]$$
$$\Big\{ \int (s/2\pi)^2 \mathrm{d}\alpha''_1 \mathrm{d}\alpha''_2 \exp[-\mathrm{i}s\, \alpha''_\sigma x_\sigma]\ \exp[-s\, \gamma^0(x_3 - \Delta x_3, \alpha''_\nu)\, \Delta x_3]\ \exp[\mathrm{i}s\, \alpha''_\sigma x'_\sigma]$$
$$-s\varepsilon\, \xi^{[1]}_{[1]}(x_\mu, x_3 - \tfrac{1}{2}\Delta x_3)\, \Delta x_3 \int (s/2\pi)^2 \mathrm{d}\alpha''_1 \mathrm{d}\alpha''_2 \exp[-\mathrm{i}s\, \alpha''_\sigma x_\sigma] \qquad (5.41)$$
$$\exp[-s\, \gamma^0(x_3 - \Delta x_3, \alpha''_\nu)\, \Delta x_3]\ [a^{[1]}_{[1]}(x_3 - \tfrac{1}{2}\Delta x_3, \alpha''_\nu) - a^{[1]}_{[1]}(x_3 - \tfrac{1}{2}\Delta x_3, 0)]\ \exp[\mathrm{i}s\, \alpha''_\sigma x'_\sigma] \Big\}$$

which, switching from left to right symbols (cf. Eq.(eq:4.132L)), can also be written as

$$\int \mathrm{d}x'_1 \mathrm{d}x'_2 \hat{g}^{(+)}(x_\mu, x_3; x'_\nu, x_3 - \Delta x_3)(\cdot) \simeq \int (s/2\pi)^2 \mathrm{d}\alpha''_1 \mathrm{d}\alpha''_2$$
$$\exp[-\mathrm{i}s\, \alpha''_\sigma x_\sigma] \exp[-s\, \gamma^0(x_3 - \Delta x_3, \alpha''_\nu)\, \Delta x_3]\, \mathcal{N}_{\alpha''_\nu, \Delta x_3}$$
$$\Big\{ \int \mathrm{d}x'_1 \mathrm{d}x'_2 \exp[\mathrm{i}s\, \alpha''_\sigma x'_\sigma]\ \exp[-s\varepsilon\, \xi^{[1]}_{[1]}(x'_\nu, x_3 - \tfrac{1}{2}\Delta x_3) a^{[1]}_{[1]}(x_3 - \tfrac{1}{2}\Delta x_3, 0)\ \Delta x_3]\,(\cdot)$$
$$-s\, \Delta x_3\ [a^{[1]}_{[1]}(x_3 - \tfrac{1}{2}\Delta x_3, \alpha''_\nu) - a^{[1]}_{[1]}(x_3 - \tfrac{1}{2}\Delta x_3, 0)] \int \mathrm{d}x'_1 \mathrm{d}x'_2 \qquad (5.42)$$
$$\exp[\mathrm{i}s\, \alpha''_\sigma x'_\sigma]\, \varepsilon\, \xi^{[1]}_{[1]}(x'_\nu, x_3 - \tfrac{1}{2}\Delta x_3)\ \exp[-s\varepsilon\, \xi^{[1]}_{[1]}(x'_\nu, x_3 - \tfrac{1}{2}\Delta x_3) a^{[1]}_{[1]}(x_3 - \tfrac{1}{2}\Delta x_3, 0)\ \Delta x_3](\cdot) \Big\}$$

In this expression we have introduced a (windowed) normalizing operator $\mathcal{N}$ to restore the appropriate amplitude behavior which was destroyed by the Taylor expansion of the exponential in Eq.(5.40),

$$\mathcal{N}\{y(1 + p + \mathrm{i}q)\} = y \exp(\mathrm{i}q)\ \left| 1 + \frac{p}{1 + \mathrm{i}q} \right|^{-1} \left[1 + \frac{p}{1 + \mathrm{i}q} \right]\ ,\quad |y| = 1\ .$$

Every additional order in the generalized-screen expansion (5.27), in Eq.(5.41) requires an additional inverse Fourier transform. The phase-screen approximation is obtained by omitting the second terms – proportional to Δx_3 – in expressions (5.41), (5.42). The numerical procedure is discussed in Le Rousseau and De Hoop [35] and is illustrated in Figure 5.5. This figure is the counterpart of Figure 5.4.

The key simplification of the 'exact' thin-slab propagator accomplished by the (generalized) screen approximation is, that the inverse (scaled) Fourier transforms with respect to α''_ν

no longer have to be evaluated for each x_μ *separately*; compare Eq.(5.41) with Eq.(3.9). This feature was inherited from the split-step Fourier or phase-screen approach, and also appears in the action of the pseudo-differential operators involved in the Bremmer series computation. The functions $\overset{\lambda^{[n]}}{\xi}_{[1-m]}(x_\mu)$ in Eq.(5.29) constitute the generalized screen, while the functions $\overset{\lambda^{[n]}}{a}_{[1-m]}(\alpha_\nu)$ extend the 'phase shift', see Figure 5.1. Further, we note that the concept of generalized screen has been inspired by the Rytov approximation.

In Eq.(5.41) we recognize the Laplace-domain Green's functions in the background medium,

$$\int (s/2\pi)^2 \mathrm{d}\alpha_1'' \mathrm{d}\alpha_2'' \exp[-s\,\{\mathrm{i}\alpha_\sigma''(x_\sigma - x_\sigma') + \gamma^0(x_3 - \Delta x_3, \alpha_\nu'')\,\Delta x_3\}]$$

[the pressure response due to a vertical point force] and

$$\int (s/2\pi)^2 \mathrm{d}\alpha_1'' \mathrm{d}\alpha_2''\, a^{[1]}_{[1]}(x_3 - \tfrac{1}{2}\Delta x_3, \alpha_\nu'')\ \exp[-s\,\{\mathrm{i}\alpha_\sigma''(x_\sigma - x_\sigma') + \gamma^0(x_3 - \Delta x_3, \alpha_\nu'')\,\Delta x_3\}]$$

[the pressure response due to a point injection source]. This is no surprise, as is illucidated in Appendix A. With the aid of the Cagniard-De Hoop method (see, for example, Achenbach [36]), the transformation of those functions back to the time domain can be carried out analytically. (Such a procedure was carried out for the paraxial approximations by De Hoop and De Hoop [14].) The (space-)time domain expression for $\hat{g}^{(+)}$ can then be obtained also, using the facts that multiplication by the exponential in the first line of Eq.(5.41) transforms into a time shift, whereas multiplication by s in the third line becomes a time differentiation.

The windowed screen propagator

To improve the accuracy of our propagator for a given order, we briefly consider the extension of the generalized-screen approach based on a single reference or background medium to one with multiple reference media. Thus, per window, the medium contrast is reduced. To this end, we will have to localize our analysis in the horizontal directions. For this we will employ the windowed Fourier transform:

$$\int \mathrm{d}x_1' \mathrm{d}x_2'\ \exp[\mathrm{i}s\,\alpha_\sigma'' x_\sigma']\ \chi(x_\nu' - \overline{x_\nu})$$

with the associated inverse transform

$$\int \mathrm{d}\overline{x_1} \mathrm{d}\overline{x_2}\,\chi^*(x_\nu - \overline{x_\nu})\ \int (s/2\pi)^2 \mathrm{d}\alpha_1'' \mathrm{d}\alpha_2''\ \exp[-\mathrm{i}s\,\alpha_\sigma'' x_\sigma]$$

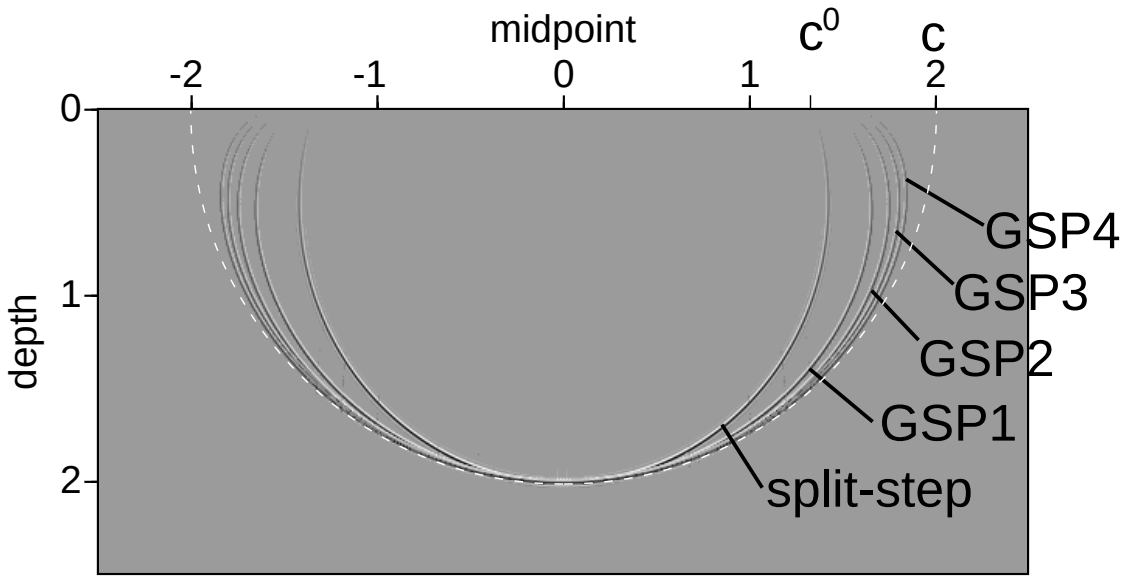

Figure 5.5: Wavefield snapshots associated with the various generalized-screen approximations.

such that

$$\int \mathrm{d}\overline{x_1}\mathrm{d}\overline{x_2}\,|\chi(x_\nu-\overline{x_\nu})|^2=1\ .$$

Equation (5.42) in windowed form, for example, becomes

$$\int \mathrm{d}x_1'\mathrm{d}x_2'\hat{g}^{(+)}(x_\mu,x_3;x_\nu',x_3-\Delta x_3)(\cdot)\simeq$$

$$\int \mathrm{d}\overline{x_1}\mathrm{d}\overline{x_2}\,\chi^*(x_\nu-\overline{x_\nu})\ \int (s/2\pi)^2\mathrm{d}\alpha_1''\mathrm{d}\alpha_2''\ \exp[-\mathrm{i}s\,\alpha_\sigma''x_\sigma]$$

$$\exp[-s\,\gamma^0(x_3-\Delta x_3,\alpha_\nu'')\,\Delta x_3]\mathcal{N}_{\alpha_\nu'',\Delta x_3}\Big\{\int \mathrm{d}x_1'\mathrm{d}x_2'$$

$$\chi(x_\nu'-\overline{x_\nu})\exp[\mathrm{i}s\,\alpha_\sigma''x_\sigma']\ \exp[-s\varepsilon\,\xi^{[1]}_{[1]}(x_\nu',x_3-\tfrac{1}{2}\Delta x_3)a^{[1]}_{[1]}(x_3-\tfrac{1}{2}\Delta x_3,0)\,\Delta x_3]\,(\cdot)$$

$$-s\,\Delta x_3\ [a^{[1]}_{[1]}(x_3-\tfrac{1}{2}\Delta x_3,\alpha_\nu'')-a^{[1]}_{[1]}(x_3-\tfrac{1}{2}\Delta x_3,0)]\int \mathrm{d}x_1'\mathrm{d}x_2'\chi(x_\nu'-\overline{x_\nu})\exp[\mathrm{i}s\,\alpha_\sigma''x_\sigma']$$

$$\varepsilon\,\xi^{[1]}_{[1]}(x_\nu',x_3-\tfrac{1}{2}\Delta x_3)\ \exp[-s\varepsilon\,\xi^{[1]}_{[1]}(x_\nu',x_3-\tfrac{1}{2}\Delta x_3)a^{[1]}_{[1]}(x_3-\tfrac{1}{2}\Delta x_3,0)\ \Delta x_3](\cdot)\Big\}$$

Each window is associated with a particular reference medium.

The P(hase) S(hift) P(lus) I(nterpolation) propagator

If, in each window, the medium is supposed to be *constant*, and if the windowing is replaced by interpolation, we recover the P(hase) S(hift) P(lus) I(nterpolation) procedure [34]. Let us return to the thin-slab propagator in Eq.(3.9). In PSPI we restrict our vertical slowness left symbol to its principal part (cf. Eq.(5.27)),

$$\hat{\gamma}^{(+)}(x_\mu, x_3-\tfrac{1}{2}\Delta x_3, \alpha''_\nu) \sim \hat{\gamma}_1(x_\mu, x_3-\tfrac{1}{2}\Delta x_3, \alpha''_\nu) = \sqrt{\hat{\mathrm{a}}^0_2(x_3-\Delta x_3, \alpha''_\nu) + \hat{\mathrm{a}}^1_2(x_\mu, x_3-\tfrac{1}{2}\Delta x_3)}$$

whereas we sample the thin-slab propagator at the coordinate values $\{x^{(i)}_\mu\}^I_{i=1}$ such that the set $\{\hat{\gamma}_1(x^{(i)}_\mu, x_3-\frac{1}{2}\Delta x_3, 0)\}^I_{i=1}$ regularly samples the range of medium velocities encountered across the current slab. Let

$$\hat{g}^{(i)}(x_3; x'_\nu, x_3-\Delta x_3) = \int (s/2\pi)^2 \mathrm{d}\alpha''_1 \mathrm{d}\alpha''_2$$

$$\exp[-\mathrm{i}s\,\alpha''_\sigma(x^{(i)}_\sigma - x'_\sigma)] \exp[-s\,\hat{\gamma}_1(x^{(i)}_\mu, x_3-\tfrac{1}{2}\Delta x_3, \alpha''_\nu)\Delta x_3]\,, \qquad (5.43)$$

which are simply homogeneous medium propagators. The thin-slab propagator $\hat{g}^{(+)}(., x_3; x'_\nu, x'_3)$ at any x_μ is then obtained by carrying out an interpolation based on $\{\hat{g}^{(i)}\}^I_{i=1}$.

6 Screen representations of the (de)composition operators

The composition operator

For the generalized-screen expansion of the composition operator (cf. Eq.(2.19)) we have to expand (the symbol of) the vertical slowness operator itself. The action of the vertical slowness operator $\hat{\Gamma}^{(+)}$ can be cast in a form compatible with the thin-slab propagator (Eq.(5.39)) and represented by its Schwartz kernel [37] $\hat{\mathcal{C}}^{(+)}$, obtained from the left symbol $\hat{\gamma}^{(+)}$ through the inverse Fourier transforms,

$$\hat{\mathcal{C}}^{(+)}(x_\mu, x'_\nu; x_3) = \int (s/2\pi)^2 \mathrm{d}\alpha''_1 \mathrm{d}\alpha''_2\, \exp[-\mathrm{i}s\,\alpha''_\sigma(x_\sigma - x'_\sigma)]\, \hat{\gamma}^{(+)}(x_\mu, x_3, \alpha''_\nu)\,. \qquad (6.1)$$

In accordance with Eq.(5.42) the Schwartz kernel for the vertical slowness is thus approximated by

$$\hat{\mathcal{C}}^{(+)}(x_\mu, x'_\nu; x_3) \simeq \int (s/2\pi)^2 \mathrm{d}\alpha''_1 \mathrm{d}\alpha''_2 \exp[-\mathrm{i}s\,\alpha''_\sigma x_\sigma]\, \gamma^0(x_3, \alpha''_\nu)\, \exp[\mathrm{i}s\,\alpha''_\sigma x'_\sigma]$$

$$+\varepsilon\, \xi^{[1]}_{[1]}(x_\mu, x_3)\, a^{[1]}_{[1]}(x_3, 0)\, \delta(x_\mu - x'_\mu) \qquad (6.2)$$

$$+\varepsilon\, \xi^{[1]}_{[1]}(x_\mu, x_3) \int (s/2\pi)^2 \mathrm{d}\alpha''_1 \mathrm{d}\alpha''_2 \exp[-\mathrm{i}s\,\alpha''_\sigma x_\sigma][a^{[1]}_{[1]}(x_3, \alpha''_\nu) - a^{[1]}_{[1]}(x_3, 0)]\, \exp[\mathrm{i}s\,\alpha''_\sigma x'_\sigma]\,.$$

Switching from left to right symbols yields

$$\hat{\mathcal{C}}^{(+)}(x_\mu, x'_\nu; x_3) \simeq \int (s/2\pi)^2 \mathrm{d}\alpha''_1 \mathrm{d}\alpha''_2 \exp[-\mathrm{i}s\,\alpha''_\sigma x_\sigma]\,\gamma^0(x_3,\alpha''_\nu)\ \exp[\mathrm{i}s\,\alpha''_\sigma x'_\sigma]$$

$$+\varepsilon\,\xi^{[1]}_{[1]}(x_\mu,x_3)\,a^{[1]}_{[1]}(x_3,0)\,\delta(x_\mu - x'_\mu) \tag{6.3}$$

$$+\int (s/2\pi)^2 \mathrm{d}\alpha''_1 \mathrm{d}\alpha''_2 \exp[-\mathrm{i}s\,\alpha''_\sigma x_\sigma][a^{[1]}_{[1]}(x_3,\alpha''_\nu) - a^{[1]}_{[1]}(x_3,0)]\,\varepsilon\,\xi^{[1]}_{[1]}(x'_\nu,x_3)\ \exp[\mathrm{i}s\,\alpha''_\sigma x'_\sigma]\ .$$

In the wide-angle approximation, we substitute Eq.(5.31) in the equations above. With optimization it would be Eq.(5.35) or Eq.(5.36). Every additional order requires an additional inverse Fourier transform.

The phase-screen approximation is obtained by omitting the third terms on the right-hand sides of Eqs.(6.2)-(6.3).

The decomposition operator

The screen representation of the decomposition operator (cf. Eq.(2.20)) requires a screen approximation of the inverse vertical slowness operator. To this end, the reciprocal vertical slowness symbol must be expanded as in Eqs.(5.16)-(5.18). The reciprocal vertical slowness operator is of order -1 and hence we denote its constituent symbols as $\eta^{-1[n]}_{[-1-m]}$.

As a consequence of the expansion in ε, the constituent symbols are all separable in the phase space coordinates, x_μ and α_ν,

$$\eta^{-1[n]}_{[-1-m]}(x_\mu,\alpha_\nu) = \sum_\lambda \overset{\lambda}{\xi}{}^{-1[n]}_{[-1-m]}\,(x_\mu)\ \overset{\lambda}{a}{}^{-1[n]}_{[-1-m]}\,(\alpha_\nu)\ , \qquad m = 0,1,\cdots \tag{6.4}$$

(If $n = 1$ and $m = 0$ we have one term only in which case we omit the λ.) The expansion for the reciprocal vertical slowness left symbol up to $\mathcal{O}(\Omega^0)$ (the principal parts) follows the series

$$\frac{1}{\hat{\gamma}_1} = \frac{1}{\sqrt{\hat{\mathrm{a}}^0_2 + \hat{\mathrm{a}}^1_2}} = \frac{1}{\gamma^0\sqrt{1+(\hat{\mathrm{a}}^1_2/\hat{\mathrm{a}}^0_2)}} \sim \frac{1}{\gamma^0} + \sum_{n=1}^{\infty} \varepsilon^n\,\eta^{-1[n]}_{[-1]}\ . \tag{6.5}$$

Up to $\mathcal{O}(\varepsilon)$ we arrive at the wide-angle approximation,

$$\eta^{-1[1]}_{[-1]}(x_\mu,\alpha_\nu) = \xi^{-1[1]}_{[-1]}(x_\mu)\,a^{-1[1]}_{[-1]}(\alpha_\nu)\ , \qquad \xi^{-1[1]}_{[-1]} = -\tfrac{1}{2}\hat{\mathrm{a}}^1_2\ , \qquad a^{-1[1]}_{[-1]} = \frac{1}{(\gamma^0)^3}\ . \tag{6.6}$$

Carrying out a Taylor series expansion about $\alpha_\nu = 0$ to zero order yields

$$a^{-1[1]}_{[-1]}(\alpha_\nu) \simeq a^{-1[1]}_{[-1]}(0) = (c^0)^3\ , \tag{6.7}$$

which leads to the phase-screen or split-step approximation.

In analogy with Eq.(6.5), the $\mathcal{O}(\Omega)$ correction term is found to be [1, Section VIII]

$$-\frac{1}{2\,[\hat{\mathrm{a}}_2^0+\hat{\mathrm{a}}_2^1]^{5/2}}\left[\hat{\mathrm{a}}_1^1\,[\hat{\mathrm{a}}_2^0+\hat{\mathrm{a}}_2^1]+\tfrac{3}{2}\mathrm{i}\alpha_\sigma(D_{x_\sigma}\hat{\mathrm{a}}_2^1)\right] \tag{6.8}$$

$$=-\frac{1}{2(\gamma^0)^5\,[1+(\hat{\mathrm{a}}_2^1/\hat{\mathrm{a}}_2^0)]^{5/2}}\left[(\gamma^0)^2\hat{\mathrm{a}}_1^1\,[1+(\hat{\mathrm{a}}_2^1/\hat{\mathrm{a}}_2^0)]+\tfrac{3}{2}\mathrm{i}\alpha_\sigma(D_{x_\sigma}\hat{\mathrm{a}}_2^1)\right]\sim\sum_{n=1}^{\infty}\varepsilon^n\eta_{[-2]}^{-1[n]}\,.$$

Up to $\mathcal{O}(\varepsilon)$ we get

$$\eta_{[-2]}^{-1[1]}=-\tfrac{1}{2}\hat{\mathrm{a}}_1^1\,\frac{1}{(\gamma^0)^3}-\tfrac{3}{4}(D_{x_\sigma}\hat{\mathrm{a}}_2^1)\,\frac{\mathrm{i}\alpha_\sigma}{(\gamma^0)^5}\,, \tag{6.9}$$

which extends the wide-angle approximation Eq.(6.6).

The Schwartz kernel of the inverse vertical slowness operator has a representation as in Eq.(6.2) or (6.3).

7 Screen representations of the reflection/transmission operators

The interaction operator in Eqs.(2.22)-(2.23) allows a screen representation as well. The interaction operator consists of a superposition of contributions from the density variations and the vertical wave slowness variations.

The symbol of the multiplication operator $\frac{1}{2}\hat{A}_{1,2}^{-1}(\partial_3\hat{A}_{1,2})$ (density variation) on the right-hand side of Eq.(2.23) follows as

$$\frac{1}{2\rho}\,(\partial_3\rho)=\varepsilon\,\frac{1}{2\,(1+\varepsilon\,\mathtt{e}_\rho)}\,(\partial_3\mathtt{e}_\rho)\sim\tfrac{1}{2}\varepsilon\,(\partial_3\mathtt{e}_\rho)+\cdots \tag{7.1}$$

which reveals an inherent separation of phase space coordinates.

The symbol of the operator $\frac{1}{2}\hat{\Gamma}^{-1}(\partial_3\hat{\Gamma})$ (vertical wave slowness variation) on the right-hand side of Eq.(2.23) requires the composition of symbols

$$\tfrac{1}{2}\exp\left[-\mathrm{i}\,\partial_{\alpha'_\sigma}D_{x'_\sigma}\right]\,\hat{\gamma}^{-1}(x_\mu,x_3,\alpha'_\sigma)\,(\partial_3\hat{\gamma})(x'_\sigma,x_3,\alpha_\nu)\Big|_{(x'_\mu,\alpha'_\nu)=(x_\mu,\alpha_\nu)}\,,$$

in which we employ the expansions in accordance with Eqs.(5.29) and (6.4). The principal part is thus found to be (cf. Eqs.(5.27), (6.5))

$$\frac{1}{2\hat{\gamma}_1}\,(\partial_3\hat{\gamma}_1)=\frac{\partial_3[\hat{\mathrm{a}}_2^0+\hat{\mathrm{a}}_2^1]}{4\hat{\mathrm{a}}_2^0\,[1+(\hat{\mathrm{a}}_2^1/\hat{\mathrm{a}}_2^0)]}\sim\frac{\partial_3[\hat{\mathrm{a}}_2^0+\hat{\mathrm{a}}_2^1]}{4(\gamma^0)^2}\left[1-(\hat{\mathrm{a}}_2^1/\hat{\mathrm{a}}_2^0)+\cdots\right]\,. \tag{7.2}$$

In Figure 7.1, upon applying a centered difference to the vertical derivative ∂_3, the (exact) principal part of the reflection left symbol (the left-hand side) is compared with the plane-wave reflection coefficient. In Eq.(7.2), the expansion in ε, again, reveals a separation of phase space coordinates in the constituent terms.

Carrying out a Taylor series expansion about $\alpha_\nu = 0$ to zero order yields

$$\frac{1}{4(\gamma^0)^2} \simeq \frac{(c^0)^2}{4} \,, \tag{7.3}$$

which leads to the phase-screen or split-step approximation to Eq.(7.2).

In analogy with Eq.(6.5), the $\mathcal{O}(\Omega)$ correction term is found to be

$$\frac{1}{2\,[\hat{\mathrm{a}}_2^0+\hat{\mathrm{a}}_2^1]^3}\Big[-\tfrac{1}{2}[\hat{\mathrm{a}}_2^0+\hat{\mathrm{a}}_2^1]\,(\partial_3[\hat{\mathrm{a}}_2^0+\hat{\mathrm{a}}_2^1])\,\hat{\mathrm{a}}_1^1+\tfrac{1}{2}[\hat{\mathrm{a}}_2^0+\hat{\mathrm{a}}_2^1]^2(\partial_3\hat{\mathrm{a}}_1^1)$$
$$-\mathrm{i}\alpha_\sigma(\partial_3[\hat{\mathrm{a}}_2^0+\hat{\mathrm{a}}_2^1])\,(D_{x_\sigma}\hat{\mathrm{a}}_2^1)+\tfrac{3}{4}\mathrm{i}\alpha_\sigma[\hat{\mathrm{a}}_2^0+\hat{\mathrm{a}}_2^1]\,(D_{x_\sigma}\partial_3\hat{\mathrm{a}}_2^1)\Big] \,. \tag{7.4}$$

Hence, to $\mathcal{O}(\varepsilon)$ we get

$$\frac{1}{2\,(\gamma^0)^6}\Big[-\tfrac{1}{2}(\gamma^0)^2\,(\partial_3\hat{\mathrm{a}}_2^0)\,\hat{\mathrm{a}}_1^1+\tfrac{1}{2}(\gamma^0)^4\,(\partial_3\hat{\mathrm{a}}_1^1)$$
$$-\mathrm{i}\alpha_\sigma(\partial_3\hat{\mathrm{a}}_2^0)\,(D_{x_\sigma}\hat{\mathrm{a}}_2^1)+\tfrac{3}{4}\mathrm{i}\alpha_\sigma(\gamma^0)^2\,(D_{x_\sigma}\partial_3\hat{\mathrm{a}}_2^1)\Big] \tag{7.5}$$

which extends the wide-angle approximation (leading order in Eq.(7.2)). In Appendix B the relation between the transmission symbol and the wide-angle screen correction to the vertical slowness symbol is discussed.

The screen reflection kernel

The Schwartz kernel of the interaction operator has a representation as in Eq.(6.2) or (6.3). As in the subsection on the screen propagator, we will show the representation of the screen reflection kernel explicitly for the principal symbol, up to the second order in ε.

As in Eq.(5.40), we separate the contribution to the kernel from the symbol at 'vertical incidence', i.e. $\alpha_\nu'' = 0$. Thus, with (cf. Eqs.(5.4) and (5.7))

$$[\hat{\mathrm{a}}_2^0+\hat{\mathrm{a}}_2^1](x_\mu,x_3,0) = [c(x_\mu,x_3)]^{-2} \,,$$

we rewrite Eq.(7.2) in the form

$$\frac{1}{2\hat{\gamma}_1}(\partial_3\hat{\gamma}_1)(x_\mu,x_3,\alpha_\nu) \sim \frac{(\partial_3 c^{-2})(x_\mu,x_3)}{4c^{-2}(x_\mu,x_3)} + \tfrac{1}{4}(\partial_3 c^{-2})(x_\mu,x_3)$$
$$\left[\left(\frac{1}{\hat{\mathrm{a}}_2^0(x_3,\alpha_\nu)} - \frac{1}{\hat{\mathrm{a}}_2^0(x_3,0)}\right) - \hat{\mathrm{a}}_2^1(x_\mu,x_3)\left(\frac{1}{[\hat{\mathrm{a}}_2^0(x_3,\alpha_\nu)]^2} - \frac{1}{[\hat{\mathrm{a}}_2^0(x_3,0)]^2}\right) + \cdots\right] \tag{7.6}$$

In Figure 7.2, upon applying a centered difference to the vertical derivative ∂_3, the exact principal part of the reflection left symbol is compared with its first and second order generalized screen approximations, in accordance with the equation above.

The Schwartz kernel then follows as (cf. Eq.(6.2))

$$\hat{\mathcal{R}}(x_\mu,x'_\nu;x_3) \simeq \frac{(\partial_3 c^{-2})(x_\mu,x_3)}{4c^{-2}(x_\mu,x_3)}\,\delta(x_\mu-x'_\mu)$$
$$+\tfrac{1}{4}(\partial_3 c^{-2})(x_\mu,x_3)\int (s/2\pi)^2 \mathrm{d}\alpha''_1\mathrm{d}\alpha''_2 \exp[-\mathrm{i}s\,\alpha''_\sigma x_\sigma]\left(\frac{1}{\hat{\mathrm{a}}_2^0(x_3,\alpha''_\nu)} - \frac{1}{\hat{\mathrm{a}}_2^0(x_3,0)}\right)\exp[\mathrm{i}s\,\alpha''_\sigma x'_\sigma]$$
$$-\tfrac{1}{4}(\partial_3 c^{-2})(x_\mu,x_3)\,\hat{\mathrm{a}}_2^1(x_\mu,x_3)\int (s/2\pi)^2 \mathrm{d}\alpha''_1\mathrm{d}\alpha''_2 \exp[-\mathrm{i}s\,\alpha''_\sigma x_\sigma]$$
$$\left(\frac{1}{[\hat{\mathrm{a}}_2^0(x_3,\alpha''_\nu)]^2} - \frac{1}{[\hat{\mathrm{a}}_2^0(x_3,0)]^2}\right)\exp[\mathrm{i}s\,\alpha''_\sigma x'_\sigma]\,. \tag{7.7}$$

Comparison with the De Wolf approximation

According to Eq.(4.10) the leading order backscattered field is given by

$$\hat{W}_2^{(1)} = \hat{\mathrm{K}}_{2,1}\hat{W}_1^{(0)}\,, \tag{7.8}$$

which can be cast into a recursion for $\hat{I}_{2,1}^{(1)}$ using Eq.(4.25). This equation bears resemblance with the De Wolf approximation [38] though the interaction operator follows from scattering across level surfaces rather than from thin volumes. The algorithm is described by Eq.(4.27) ($J=2$) for the slab $[k\Delta x_3,(k+1)\Delta x_3]$.

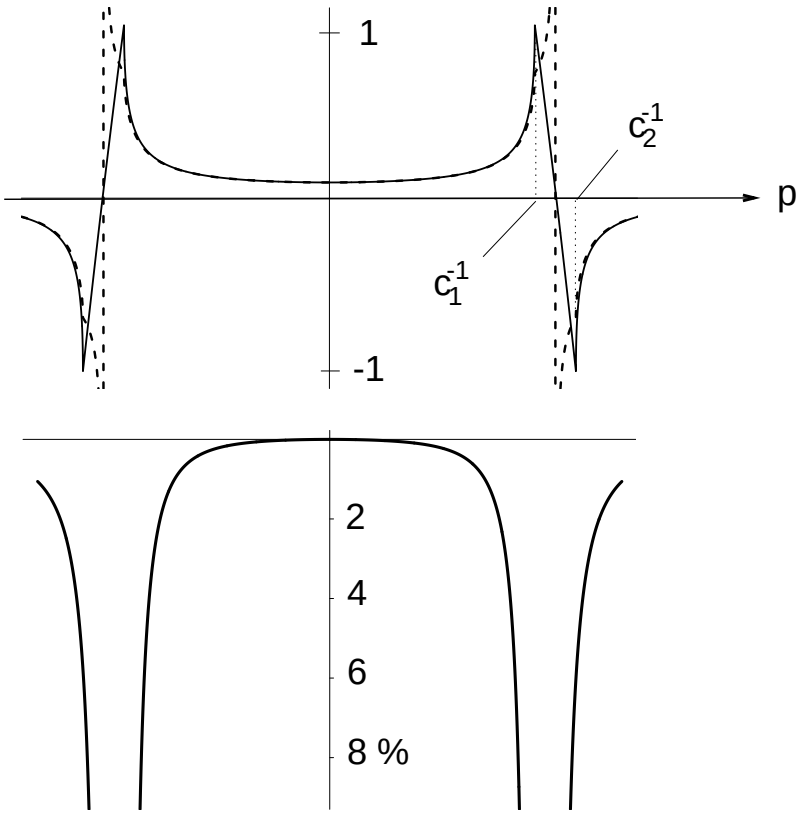

Figure 7.1: The centered difference (in x_3) representation of the principal part of the reflection symbol (dashed) and the corresponding plane-wave reflection coefficient (solid): real parts. The relative difference between the two is shown at the bottom.

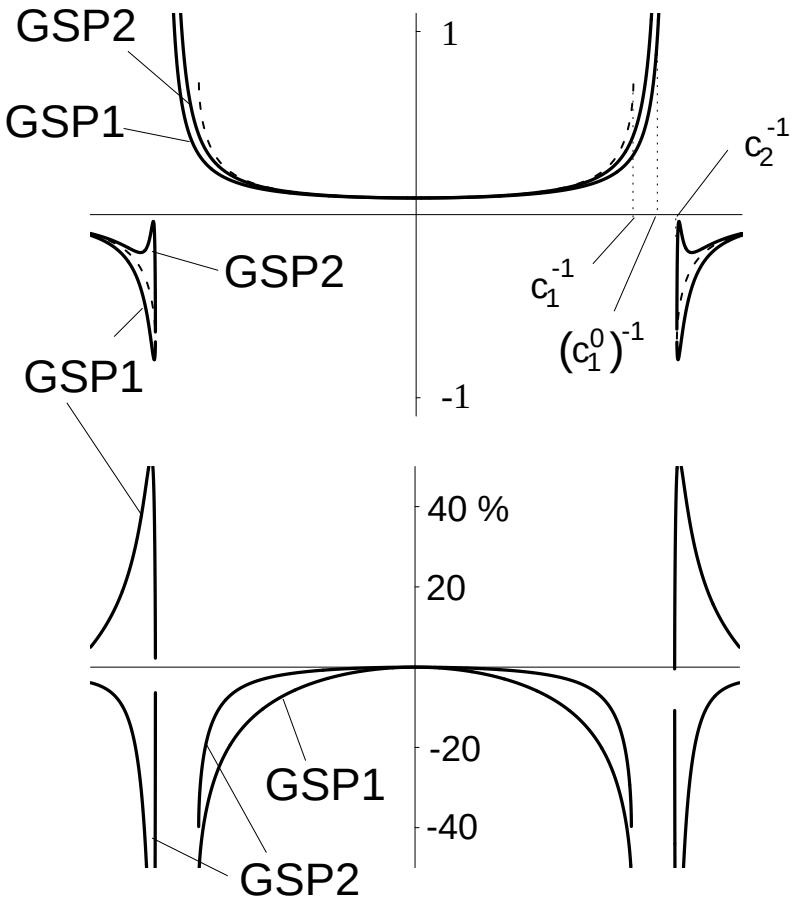

Figure 7.2: Principal parts of the generalized screen reflection left symbols: first order (GSP1) and second order (GSP2). The exact reflection symbol is dashed. The relative differences between the generalized screen and the exact reflection symbols are shown in the bottom part.

8 Concluding remarks

We have developed a class of screen-like algorithms for the multi-dimensional (generalized) Bremmer coupling series. The key ingredient was a separation of variables of the vertical slowness in horizontal phase space. This separation originated from an embedding procedure and an expansion of all relevant quantities in magnitude and smoothness of the medium contrast with respect to the embedding. Our scheme has added to the standard phase-screen method in the following ways: we considered larger medium variations in the lateral directions; we enhanced the accuracy for larger scattering angles; we introduced (de)composition operators to incorporate any desired source- or receiver-type with the appropriate radiation characteristics; we have taken care of the backscattered field with the aid of the Bremmer coupling series. The backscattered field includes phenomena like turning ray waves; the screen propagator accounts for focussing and defocussing effects also. The screen approximation, however, does not model critical-angle phenomena such as head waves, though it captures some of the evanescent wave contributions.

The methodology followed in this paper provides a platform from which one can evaluate the generalized-screen expansion for wave propagation and scattering up to any desired level of accuracy. However, the validity of the methodology is restricted to the time-Laplace domain. Termwise, with the aid of complex analysis, the generalized-screen expansion can be reformulated and given appropriate meaning in the time-Fourier domain – taking special care of the branch cuts associated with the vertical wave slowness in the embedding.

Not only have we investigated the accuracy of the generalized-screen approximations on the wavefront using the locally frozen values for medium properties; we have analyzed the influence of the rate of change of the medium properties also. Our formulae can be used to quantify the leading-order contribution to the scattering process due to those rates.

The computational complexity of our algorithm is given by $(2+m)\,(N\log N+N)$ where m is the order of the generalized-screen approximation, and N is the number of nodes at which the wavefield is sampled in the horizontal directions, multiplied by the number of vertical steps and by the number of terms in the Bremmer series. In principle, this complexity is comparable to the one associated with the P(arabolic) E(quation) algorithms. However, *implicit*, stable PE algorithms require the solution of a (sparse) system of equations at each vertical propagation step. Whatever method used, in three dimensions, the computational complexity of the solution procedure will be greater than the one of the generalized-screen approach.

There are various fields of application of the method presented in this paper. One concerns the numerical implementation of wave equation solvers in acoustics and electromagnetics.

Some, benchmark numerical results have been published by Le Rousseau and De Hoop [39]. Otherwise, in the study of propagation of waves in smoothly varying random media, the method has been proven to be useful. Finally, the lowest order approximations discussed in this paper have already found application in seismic imaging [40, 41, 42]. A first step towards extending the procedure to elasticity can be found in [43].

Acknowledgment

The authors would like to thank Mobil and Elf Exploration Production for financial support of this research. The authors would also like to thank Douglas Foster and Michael Fehler for many valuable discussions.

Appendix A. Comparison of the wide-angle-screen with the local-Born approximations

Dividing up the propagation range into thin slabs, and applying a Born approximation to each of them, Wu and Huang [13] found the following spectral-domain propagator,

$$\tilde{g}^{(+)}(\alpha_\mu, x_3; \alpha'_\nu, x'_3) \simeq \exp[-s\gamma^0(x_3,\alpha_\mu)x_3] \tag{A.1}$$

$$\left\{\delta(\alpha_\mu-\alpha'_\mu)+\frac{(-s)}{2\,[c^0(x_3)]^2\gamma^0(x_3,\alpha_\mu)}\,\Delta x_3\,\tilde{\mathsf{f}}(\alpha_\mu,x_3,\alpha'_\nu,x'_3)\right\}\exp[s\gamma^0(x_3,\alpha'_\nu)x'_3]\ ,$$

where

$$\tilde{\mathsf{f}}(\alpha_\mu,x_3,\alpha'_\nu,x'_3) = -\tilde{\tilde{\epsilon}}_\kappa(\alpha_\mu-\alpha'_\mu,\gamma^0(x_3,\alpha_\mu)-\gamma^0(x_3,\alpha'_\nu)) \tag{A.2}$$

$$+[c^0(x_3)]^2[\alpha_\sigma\alpha'_\sigma+\gamma^0(x_3,\alpha_\mu)\gamma^0(x_3,\alpha'_\nu)]\,\tilde{\tilde{\epsilon}}_\rho(\alpha_\mu-\alpha'_\mu,\gamma^0(x_3,\alpha_\mu)-\gamma^0(x_3,\alpha'_\nu))\ ,$$

arising from the contrast-source radiation patterns, and in which

$$\tilde{\tilde{\epsilon}}_\kappa=\frac{1}{\Delta x_3}\int_{\zeta=x'_3}^{x_3}\mathrm{d}\zeta\ \exp[\mathrm{i}s\alpha_3\zeta]\,\tilde{\epsilon}_\kappa(\alpha_\mu,\zeta)\ ,\quad \tilde{\tilde{\epsilon}}_\rho=\frac{1}{\Delta x_3}\int_{\zeta=x'_3}^{x_3}\mathrm{d}\zeta\ \exp[\mathrm{i}s\alpha_3\zeta]\,\tilde{\epsilon}_\rho(\alpha_\mu,\zeta) \tag{A.3}$$

are windowed Fourier transforms with respect to the vertical coordinate.

Applying a lowest order *difference* paraxial approximation to the perturbation term in the thin slab propagator, viz.,

$$\gamma^0(x_3,\alpha_\mu)-\gamma^0(x_3,\alpha'_\mu) \;=\; \mathcal{O}(\alpha_\mu-\alpha'_\mu)\ , \tag{A.4}$$

$$\alpha_\sigma\alpha'_\sigma+\gamma^0(x_3,\alpha_\mu)\gamma^0(x_3,\alpha'_\nu) \;=\; [c^0(x_3)]^{-2}+\mathcal{O}(\alpha_\mu-\alpha'_\mu)\ , \tag{A.5}$$

we arrive at

$$\tilde{\mathsf{f}}\simeq\tilde{\tilde{\epsilon}}_\rho(\alpha_\mu-\alpha'_\mu,0)-\tilde{\tilde{\epsilon}}_\kappa(\alpha_\mu-\alpha'_\mu,0)\ . \tag{A.6}$$

Upon comparing now the spectral-domain propagator with Eqs.(3.13)-(3.13), we find an expression,

$$\gamma^0(x_3,\alpha_\mu)+\frac{1}{\gamma^0(x_3,\alpha_\mu)}\,\frac{\tilde{\mathsf{f}}(\alpha_\mu,x_3,\alpha'_\nu,x'_3)}{2\,[c^0(x_3)]^2}\ .$$

which, in view of Eq.(A.4), is directly related to the cokernel (Eq.(5.30)) associated with the wide-angle approximation Eq.(5.31). Out of the expression for the cokernel, we can extract the screen $S_{c^{-1}}$ (cf. Eq.(5.13))

$$\tilde{\gamma}(\alpha_\mu-\alpha'_\mu,x_3-\tfrac{1}{2}\Delta x_3,\alpha'_\nu,s)\simeq\gamma^0(x_3,\alpha'_\nu)+\frac{1}{\gamma^0(x_3,\alpha'_\nu)}\,\frac{\tilde{S}_{c^{-1}}(\alpha_\mu-\alpha'_\mu,x_3)}{[c^0(x_3)]^2}\ . \tag{A.7}$$

Appendix B. Comparison of the wide-angle-screen approximation with linearized transmission coefficients

To account for horizontal medium variations, we introduced the leading-order scattering correction Eq.(5.31):

$$\hat{\gamma}_1 - \gamma^0 \sim \frac{\hat{\mathrm{a}}_2^1}{2\,\gamma^0} \sim 2\gamma^0\,\frac{(c^0)^{-1}\epsilon_{c^{-1}}}{2c^0\,(\gamma^0)^2}\ . \tag{B.1}$$

In comparison, the scattering due to vertical medium variations is given by Eq.(7.2), i.e.,

$$\frac{1}{2\hat{\gamma}_1}\,(\partial_3\hat{\gamma}_1) \sim \frac{\partial_3[\hat{\mathrm{a}}_2^0 + \hat{\mathrm{a}}_2^1]}{4\,(\gamma^0)^2} \sim \frac{(\partial_3 c^{-1})}{2c^0\,(\gamma^0)^2}\ , \tag{B.2}$$

which constitutes the linearized transmission(/reflection) coefficient.

Upon discretizing the vertical derivative, the two expressions above become directly related.

References

[1] M.V. de Hoop, "Generalization of the Bremmer coupling series," *J. Math. Phys. 37*, 3246-3282 (1996).

[2] M.V. de Hoop, "Direct, leading-order asymptotic, inverse scattering based on the generalized Bremmer series," in *Mathematical and numerical aspects of wave propagation*, ed. J.A. DeSanto, pp.249-253, SIAM (1998).

[3] F.D. Tappert, "The parabolic approximation method," in *Wave propagation and underwater acoustics*, eds. J.B. Keller and J.S. Papadakis, pp.224-287, Lecture Notes in Physics Vol.70, Springer-Verlag, New York (1977).

[4] M.D. Collins, "Applications and time-domain solution of higher-order parabolic equations in underwater acoustics," *J. Acoust. Soc. Am. 86*, 1097-1102 (1989).

[5] J.F. Claerbout, "Coarse grid calculations of wave in inhomogeneous media with application to delineation of complicated seismic structure," *Geoph. 35*, 407-418 (1970).

[6] G.R. Hadley, "Wide-angle beam propagation using Padé approximant operator," *Opt. Lett. 17*, 1426-1428 (1992).

[7] M.J.N. van Stralen, M.V. de Hoop and H. Blok, "Generalized Bremmer series with rational approximation for the scattering of waves in inhomogeneous media," *J. Acoust. Soc. Am. 104*, 1943-1963 (1998).

[8] B.L.N. Kennett, *Seismic wave propagation in stratified media*, Cambridge University Press, Cambridge (1985).

[9] J. Gazdag, "Wave equation migration with the phase shift method," *Geoph. 43*, 1342-1351 (1978).

[10] F. Treves, *Introduction to pseudodifferential and Fourier integral operators*, Vols. 1 and 2, Plenum Press, New York (1980).

[11] L. Fishman and J.J. McCoy, "Derivation and application of extended parabolic wave theories I. The factorized Helmholtz equation," *J. Math. Phys. 25*, 285-296 (1984).

[12] P.L. Stoffa, J.T. Fokkema, R.M. de Luna Freire and W.P. Kessinger, "Split-step Fourier migration," *Geoph. 55*, 410-421 (1990).

[13] R.-S. Wu and L.-J. Huang, "Scattered field calculation in heterogeneous media using phase-screen propagator," 62nd Ann. Mtg. Soc. Explor. Geophys., Expanded Abstracts, pp.1289-1292 (1992).

[14] M.V. de Hoop and A.T. de Hoop, "Scalar space-time waves in their spectral-domain first- and second-order Thiele approximations," *Wave Motion 15*, 229-265 (1992).

[15] L. Fishman and J.J. McCoy, "Derivation and application of extended parabolic wave theories II. Path integral representations," *J. Math. Phys. 25*, 297-308 (1984).

[16] J.J. McCoy and L.N. Frazer, "Pseudodifferential operators, operator orderings, marching algorithms and path integrals for one-way equations," *Wave Motion 9*, 413-427 (1987).

[17] J.A. Ratcliffe, "Some aspects of diffraction theory and their application to the ionosphere," *Rep. Prog. Phys. 19*, 190-263 (1956).

[18] R.P. Mercier, "Diffraction by a screen causing large random phase fluctuations," *Proc. Cambridge Philos. Soc. 58*, 382-400 (1962).

[19] J.M. Martin and S.M. Flatté, "Intensity images and statistics from numerical simulation of wave propagation in 3-D random media," *Appl. Opt. 27*, 2111-2125 (1988).

[20] M.D. Feit and J.A. Fleck, Jr., "Light propagation in graded-index optical fibers," *Appl. Opt. 17*, 3990-3998 (1978).

[21] R. Buckley, "Diffraction by a random phase-changing screen: a numerical experiment," *J. Atmos. Terr. Phys. 37*, 1431-1446 (1975).

[22] E.N. Bramley, "The accuracy of computing ionospheric radiowave scintillation by the thin-phase screen approximation," *J. Atmos. Terr. Phys. 39*, 367-373 (1977).

[23] D.L. Knepp, "Multiple phase screen calculation of the temporal behavior of stochastic waves," *Proc. IEEE 71*, 722-737 (1983).

[24] S.M. Flatté, R. Dashen, W.H. Munk, K.M. Watson and F. Zachariasen, *Sound transmission through a fluctuating ocean*, Cambridge University Press, New York (1979).

[25] D.J. Thomson and N.R. Chapman, "A wide-angle split-step algorithm for the parabolic equation," *J. Acoust. Soc. Am. 74*, 1848-1854 (1983).

[26] M.D. Fisk and G.D. McCartor, "The phase screen method for vector elastic waves," *J. Geophys. Res. 96*, 5985-6010 (1991).

[27] M.D. Fisk, E.E. Charrette and G.D. McCartor, "A comparison of phase screen and finite difference calculations for elastic waves in random media," *J. Geophys. Res. 97*, 12,409-12,423 (1992).

[28] R.-S. Wu, "Wide-angle elastic wave one-way propagation in heterogeneous media and an elastic wave complex-screen method," *J. Geophys. Res. 99*, 751-766 (1994).

[29] M.V. Berry, "Diffractals," *J. Phys. A: Math. Gen. 12*, 781-796 (1979).

[30] M.V. de Hoop and A.K. Gautesen, "Uniform asymptotic expansion of the generalized Bremmer series," *SIAM J. Appl. Math.*, in print (1999).

[31] C. De Witte-Morette, A. Maheshwari and B. Nelson, "Path integration in non-relativistic quantum mechanics," *Physics Reports 50*, 255-372 (1979).

[32] D.V. Widder, *The Laplace transform*, Princeton University Press, Princeton (1946).

[33] A.T. de Hoop, "Convergence criterion for the time-domain iterative Born approximation to scattering by an inhomogeneous, dispersive object," *J. Opt. Soc. Am. A 8*, 1256-1260 (1991).

[34] J. Gazdag and P. Sguazzero, "Migration of seismic data by phase shift plus interpolation," *Geoph. 49*, 124-131 (1984).

[35] J.H. Le Rousseau and M.V. de Hoop, "Modeling and imaging with the scalar generalized-screen algorithm in isotropic and transversely isotropic media," *Geoph.*, in print (1999).

[36] J.D. Achenbach, *Wave propagation in elastic solids*, North-Holland, Amsterdam (1973).

[37] L. Schwartz, *Théorie des distributions*, 2nd ed., Hermann, Paris (1966).

[38] R.-S. Wu and L.-J. Huang, "Reflected wave modeling in heterogeneous acoustic media using the de Wolf approximation," in *Mathematical Methods in Geophysical Imaging III*, ed. S. Hassanzadeh, pp.176-186, Proc. SPIE 2571 (1995).

[39] J.H. Le Rousseau and M.V. de Hoop, "Modeling and imaging with the generalized screen algorithm," 68th Ann. Mtg. Soc. Explor. Geophys., Expanded Abstracts, pp.1937-1940 (1998).

[40] L.-J. HUANG AND R.-S. WU, "3D prestack depth migration with acoustic pseudo-screen propagators," in *Mathematical Methods in Geophysical Imaging IV*, ed. S. Hassanzadeh, pp.40-51, Proc. SPIE 2822 (1996).

[41] R.-S. Wu and S. Jin, "Windowed GSP (generalized screen propagators) migration applied to SEG-EAEG salt model data," 67th Ann. Mtg. Soc. Explor. Geophys., Expanded Abstracts, pp.1746-1749 (1997).

[42] L.-J. Huang, M.C. Fehler and R.-S. Wu, "Extended local Born Fourier migration method," *Geoph.*, submitted (1998).

[43] R.-S. Wu and X.-B. Xie, "Multi-screen backpropagator for fast 3D elastic prestack migration," in *Mathematical Methods in Geophysical Imaging II*, ed. S. Hassanzadeh, pp.181-193, Proc. SPIE 2301 (1994).